Journal of African Earth Sciences 119 (2016) 238–255

Contents lists available at ScienceDirect

Journal of African Earth Sciences

journal homepage: www.elsevier.com/locate/jafrearsci

# Metre-scale cyclicity in Middle Eocene platform carbonates in northern Egypt: Implications for facies development and sequence stratigraphy

Mohamed Tawfik [a], Abdelbaset El-Sorogy [a, b, *], Mahmoud Moussa [c]

[a] Geology Department, Faculty of Science, Zagazig University, Zagazig, Egypt
[b] Department of Geology and Geophysics, College of Science, King Saud University, Saudi Arabia
[c] Faculty of Georesources and Materials Engineering, EMR Group, RWTH Aachen University, Germany

ARTICLE INFO

*Article history:*
Received 20 December 2015
Received in revised form
23 March 2016
Accepted 6 April 2016
Available online 12 April 2016

*Keywords:*
Facies analysis
Paleoenvironment
Middle Eocene
Cyclicity
Sequence stratigraphy
Egypt

ABSTRACT

The shallow-water carbonates of the Middle Eocene in northern Egypt represent a Tethyan reef-rimmed carbonate platform with bedded inner-platform facies. Based on extensive micro- and biofacies documentation, five lithofacies associations were defined and their respective depositional environments were interpreted. Investigated sections were subdivided into three third-order sequences, named S1, S2 and S3. Sequence S1 is interpreted to correspond to the Lutetian, S2 corresponds to the Late Lutetian and Early Bartonian, and S3 represents the Late Bartonian. Each of the three sequences was further subdivided into fourth-order cycle sets and fifth-order cycles. The complete hierarchy of cycles can be correlated along 190 km across the study area, and highlighting a general "layer-cake" stratigraphic architecture. The documentation of the studied outcrops may contribute to the better regional understanding of the Middle Eocene formations in northern Egypt and to Tethyan pericratonic carbonate models in general.



## 1. Introduction

The Eocene sediments in northern Egypt are characterized by excellent exposure and are dominated by shallow marine carbonates, characterized by large foraminifera and other fossils. From the Eastern Desert to the Western Desert in Egypt, it is notable that the Middle Eocene coral reef banks in the Eastern Desert. These corals gradually decrease towards Cairo (to the west) and become totally replaced by bryozoans, nummulite, oysters and other bivalve banks. In the Western Desert, near the Fayum province, a thick succession of clastic sediments intercalated with argillaceous limestone that is dominated by nummulite and oyster shells. According to El-Azabi (2006) the carbonate sediments of the Middle Eocene in the Eastern Desert have been deposited on an isolated shallow marine Platform (carbonate bank) with a high carbonate productivity. Deposition is thought to have occurred under a warm semi-arid climate, with seawater of normal salinity and oxygen content, and moderate to slightly restricted water circulation with the open sea.

To achieve these aims, six Middle Eocene stratigraphic sections were measured, described and examined in the region between Wadi el Ramliya (the Eastern Desert) to Wadi el Hitan (the Western Desert) (Fig. 1). The Middle Eocene in northern Egypt has been studied by numerous authors (e.g. Strougo and Boukhary, 1987; Said, 1990; Haggag, 1990, 1992; Strougo, 1985a, 1985b, 2008; Helal, 1990, 2002; Strougo and Azab, 1991; Allam et al., 1991; Gingerich, 1992; Strougo et al., 1992; Boukhary et al., 1993; Omar 1999; Uhen, 2004; Mostafa and Hassan, 2004; Lotfy and Van der Voo, 2007; Abdel-Fattah et al., 2010; Abu Elghar, 2012 El-Fawal et al., 2013, Marzouk et al., 2014 and Sallam et al, 2015a,b). This paper adopts the lithostratigraphic columns of Said (1990) and Strougo (2008). Most of the fossils identified in the paper, as well as the biostratigraphic evidence for age determination of the studied sections, have been published in the above-cited references. This paper therefore does not mainly focus on biostratigraphy of the studied section, but rather on sequence stratigraphy. The present study aims to address the changes from the east to the west and determine the paleoecology factors that have led to unique growth,

* Corresponding author. Department of Geology and Geophysics, College of Science, King Saud University, P.O Box: 2455, Riyadh, 11451, Saudi Arabia.
*E-mail addresses:* elsorogyabd@yahoo.com, asmohamed@ksu.edu.sa (A. El-Sorogy).

http://dx.doi.org/10.1016/j.jafrearsci.2016.04.006
1464-343X/

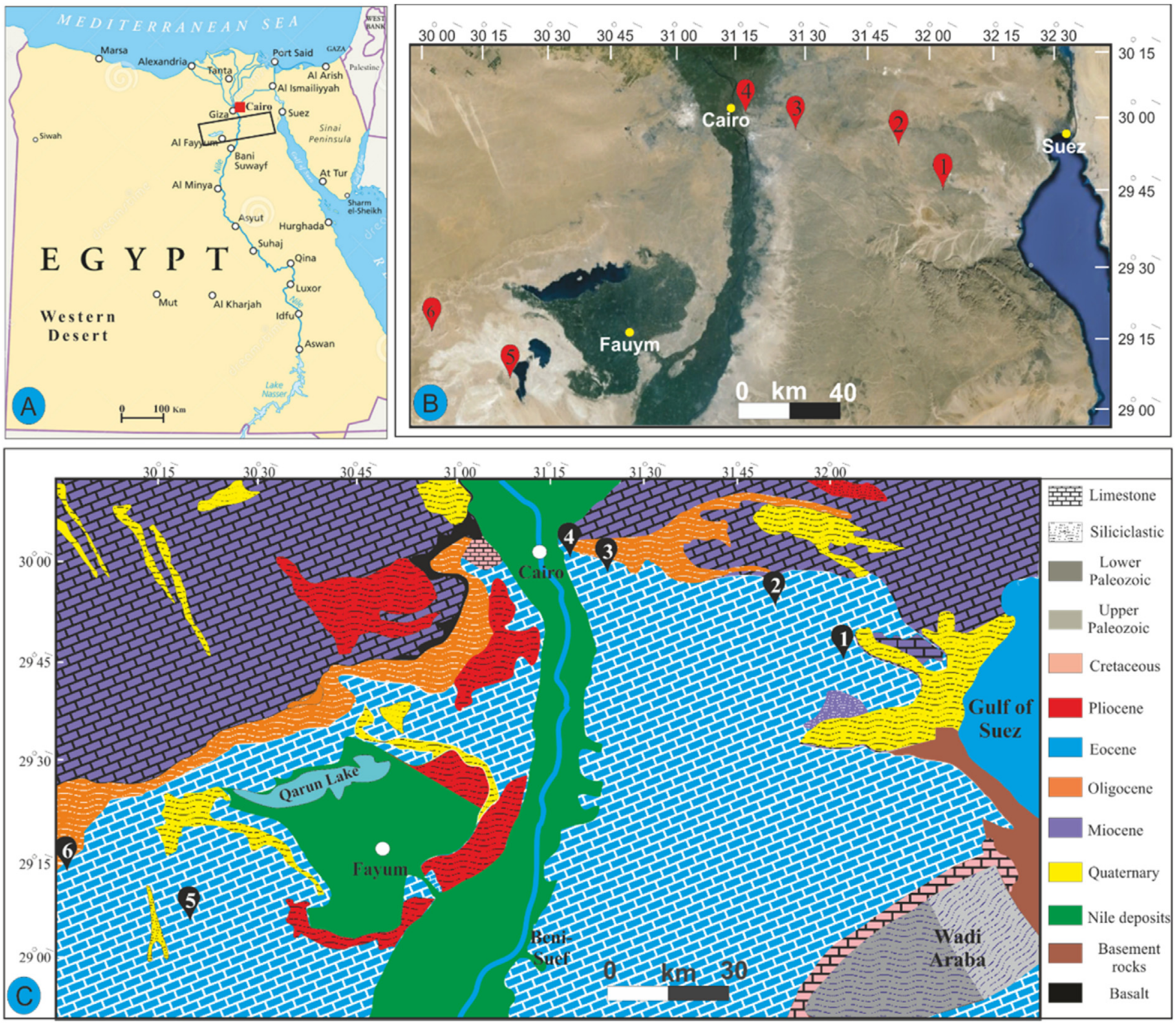


**Fig. 1.** **A**: Egypt map, **B**: Satellite image shows Middle Eocene studied sections and **C**: Geological map of northern Egypt (simplified from Egyptian geological survey, 1981).

to reset the specific depositional environments of the Eocene successions, to determine sequence boundaries and sequence stratigraphic analysis of the studied Eocene rocks, based on field and petrographic investigations. This approach makes it possible to follow the lateral facies changes and to establish a depositional model for the middle Eocene in northern Egypt.

## 2. Geological setting and tectonics

In general, the Eocene of Egypt comprises shallow-marine and marginal sediments and became shallower by the end of this period (Mansour and Holail, 2004). Said (1990) supposed that the geological history of the Egyptian Paleogene was dominated by tectonic events, which may represent an extension or rejuvenation of the Late Cretaceous tectonism. Moustafa and Khalil (1989) concluded that Egypt was greatly influenced during the Eocene by the Syrian Arc movement, the End Lutetian Pyrenean–Atlasic event in addition to the Gulf of Suez rifting initiation which resulted in the displacement of many blocks relatively to each other which gave rise to a complex stratigraphic setting on both sides of the Gulf (Steckler et al., 1988; Issawi, 2002, 2005; Osman, 2003; Issawi et al., 2009; Sallam et al., 2015a). Schandelmeier et al. (1997) have mentioned that during the Lutetian, the Alpine orogeny caused crustal shortening and the inversion of sedimentary basins in NE Africa and on the Arabian platform. The Middle Eocene development of coral reefs indicates that northern Egypt was drafted to another geographical location at lower latitudes than the recent geographic location. The growth of corals should have a tropical to subtropical climate. Lotfy and Van der Voo, 2007 studies on paleomagnetics of the marine-mammals sites and basalts in the Fayum province endorses the earlier conclusion about the Middle Eocene climate. They have determined the paleogeographic positions of Egypt at 15°–17° N, particularly during the Middle-Late Eocene interval. Such a position should suggests a possible prevalence of tropical paleogeography and paleoclimate over northeast Africa in general as well as marine mammal sites in the Fayum province as well.

Eocene sedimentation in northern parts of the Western Desert have been carried out in narrow synclinal basins, which represent arms of the Tethys Sea; created by the Late Cretaceous tectonic activity. These basins were bounded by positive landmasses that represent sites of non-deposition and/or erosion (Salem, 1976). Zalmout (2008) stated that the Fayum Basin, was a broad stable marine platform during the middle and late Eocene, following Syrian Arc rifting and compression, and preceding Red Sea rifting. The platform subsided passively, with little or no tectonic influence,

**Table 1**
Lithostratigraphic classification of the Middle- Late Eocene in northern Egypt.

**Said 1990**

| Chrono | Fayum | Gebel Mokattam | Helwan |
|---|---|---|---|
| Late | Qasr el Sagha | Maadi | Wadi Hof |
| | | | Wadi Garawi |
| | Gehannam | | Qurn |
| | Gharaq | Giushi | Observatory |
| | Sath el Hadid | | |
| | Midawara | Upper Building stone | Gebel Hof |
| | | Gizehensis | |
| | Muweilih | Lower Building stone | |
| | Samalut | | |

**Gingrich 1992**

| Chrono | NE Fayum | Cairo-Giza | Eastern Desert |
|---|---|---|---|
| Priabonian | Qasr el Sagha | Maadi | Wadi Hof/ Garawi |
| | Birket Qarun | | Qurn |
| Bartonian | Gehannam | Giushi | Observatory |
| | Midawara? | | |
| Lutetian | Wadi Rayan | Mokattam (Mo): Upper Building Stone (UBS) | Gebel Hof |
| | | Gizehensis (G) | |
| | | Lower Building Stone (LBS) | |

**Lotfy & Voo 2007**

| Chrono | | Fayum |
|---|---|---|
| Priabonian | Maadi Group | Qasr el Sagha |
| | | Birket Qarun |
| Bartonian | | Gehannam |
| Lutetian | Mokattam Group | Gharaq |
| | | Sath el Hadid |
| | | Midawara |
| | | Muweilih |
| | | Samalut |

**Strougo 2008**

| Chrono | | Fayum | N. Part of Gebel Mokattam |
|---|---|---|---|
| Priab. | Mk9 | Birket Qarun | Wadi Hof |
| Bartonian | Mk8 | Gehannam /Gharaq | Qurn |
| | Mk7 | | |
| | Mk6 | Sath el Hadid | Observatory / Giushi |
| Lutetian | Mk5 | Midawara | UBS |
| | Mk4 | | Mo: G |
| | | | LBS |
| | Mk3 | Muweilih | |
| | Mk2 | Samalut | |

**Abdel-Fattah et al. 2010**

| Chrono | Fayum |
|---|---|
| Priabonian | Qasr el Sagha |
| | Birket Qarun |
| Bartonian | Gehannam |
| Lutetian | Wadi el Rayan |

**Abu Elghar 2012**

| Chrono | Fayum Formation (Fm) | Fayum Sequence (S) |
|---|---|---|
| Priab. | Birket Qarun | |
| Bartonian | Gehannam | Sequence 4 |
| | Gharaq | Sequence 3 |
| | Sath el Hadid | |
| | Midawara | |
| Lutetian | El Muweilih | Sequence 2 |
| | Samalut | Sequence 1 |

**El-Fawal et al. 2013**

| Chrono | Fayum Fm | Fayum S |
|---|---|---|
| Priab. | Qasr el Sagha | |
| Bartonian | Birket Qarun | S2 |
| | Gehannam | S1 |

**Sallam et al. 2015b**

| Chrono | North Eastern Desert Formation |
|---|---|
| Priab. | Maadi |
| Bartonian | Qurn |
| | Observatory/ Sannor |
| | Gebel Hof |

and preserved a good record of shallow marine strata. In the North-Eastern Desert, the Middle Eocene was marked by active syn-sedimentary tectonics that resulted in many breaks and produced many different sedimentary regimes (El Ayyat, 2013). Issawi et al. (2009) have been attributed the stratigraphic and paleogeographic setting of the Cairo–Suez district during the Middle Eocene to the collision between both the African and European plates and its related impacts on the development and distribution of the different stratigraphic units in this district. The collision between the two plates produced areas of great stress, which were responsible for the breaking-up of the different stratigraphic successions on both sides of the Gulf of Suez creating many grabens, half grabens, and horst blocks of variable sizes and amplitudes (Issawi and Osman, 2002).

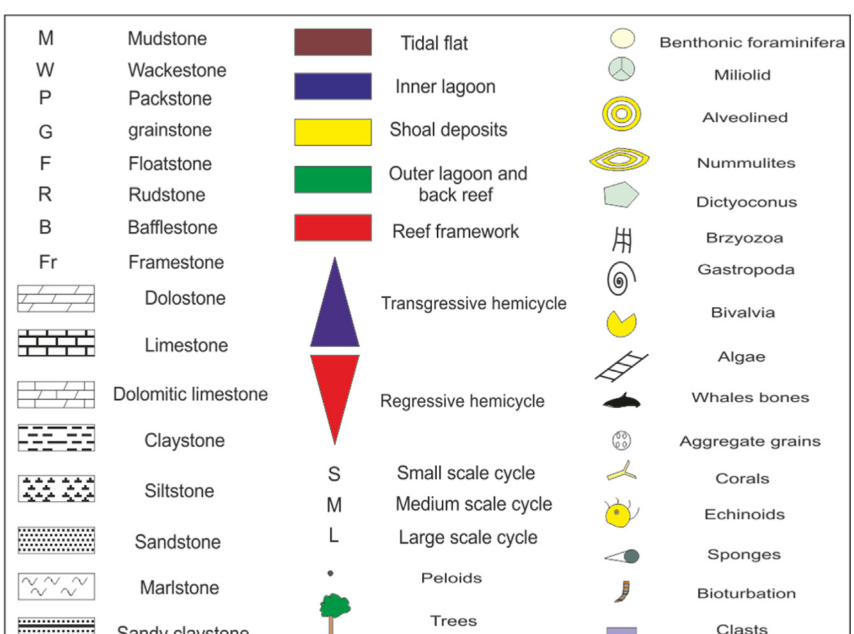


**Fig. 2.** Colour coded Texture (Embry and Klovan, 1971), Lithology, Lithofacies associations and fossils.

**Table 2**
Facies types of the Middle Eocene in northern Egypt.

| Facies types | Description | Interpretation |
|---|---|---|
| Silty claystone (1a) (Fig. 3a) | Dark grey to pale yellow-brown claystone or silty claystone, fissile gypsum filled joints, halite, carbonaceous and fragments of carbonized wood, rare shell fragments, no admixed terrigenous sand, common in Minqar el Rayan section. | The presence of halite pockets and gypsum in silty clay with no admixed terrigenous sand indicates supratidal environment. (Meckel, 1975). |
| Bioturbated calc. quartz arenite (1b) (Fig. 3b, c, d) | Yellowish white to yellow cross bedded sandstone and siltstone (at Minqar el Rayan section). Many skeletons of the marine dinosaurs and diverse fauna of sharks are represented (at Wadi el Hitan section). Burrows are common in both sections. | According to (Gingerich, 1992), the presence of vertebrate fossils indicates shallow shelf, possibly with more restricted circulation. |
| Lithoclastic bioclatstic dolostone (1c) (Fig. 3e, f) | Yellowish white to grey dolomite rhombs, rare bioclastics, quartz grains and mud clasts are recorded. It is common in the Gebel el Ramliya section. | The dolomite rhombs have been formed in the diagenetic stage as a matrix replacement. Low faunal contents imply that the parent rock was lime-mudstone that has been deposited in a tidal flat. |
| Bioclastic mudstone (2a) (Fig. 3g) | Brownish yellow lime- mudstone. It shows dm-scale low-angle lamination, contains undefined skeletal grains parallel to the bedding, shell fragments and bioturbation are common. This facies type is recorded in all sections. | The lack of mud cracks, flat lamination and birds-eye structure, indicates that the lime-mudstone was of intertidal origin and deposited in a restricted inner lagoon environment. |
| Foram. miliolid wackestone (2b) (Fig. 3h, i) | This pale yellow coloured weathered facies type shows many of foraminiferal grains as larger and small miliolids, rotaliids, orbitiolites and others. Burrows and bioturbation are observed, common in Gebel el Ramliya and Observatory sections. | The micritic texture and abundance of miliolids indicate shallow, warm, restricted quiet water. The appearance of many detrital grains in micritic texture indicates deposition near shore. |
| Bioclastic foraminiferal wacke- to packstone (2c) (Fig. 3j, k) | Pale yellow, cross to planar and flaser bedded, contains abundant orbitiolites, bivalve shells, echinoids and peloids. Neomorphism and biotic zonation are common. It is recognized in the Gebel el Ramliya, Observatory and Qattamiya sections. | The abundance of larger foraminifera may suggest that the wackestone has been formed under low to moderate circulation in the open sea. The presence of orbitiolites indicates that deposition was influenced by vegetation cover, (Hottinger, 1997). |
| Bioclastic nummulite wackestone (2d) (Fig. 3l, m) | Yellowish white, contains abundant amount of nummulite and other foraminiferal tests, bivalve shells, bryozoans and echinoid fragments. This facies type records throughout the most sections. | It indicates a back bank lagoonal facies that in a quiet, low energy regime below fair weather wave base, at 5–10 m water depth (upper subtidal). (El-Azabi, 2006). |
| Bioclastic echinoids wackestone (2e) (Fig. 3n) | Pale yellow to grey and consist mainly of echinoid fragments (esp. *Schizaster* sp.), *Nummulites*, and bivalve debris. It is recorded in the Observatory, Mokattam and Minqar el Rayan sections. | According to (Bernau et al., 2003) this facies was deposited in a low- to medium energy setting, below fwwb, in deeper subtidal lagoons in an open marine environment. |
| Bioclastic packstone (3a) (Fig. 3o) | Grey to yellowish white weathered limestone with larger and small miliolids, *Nummulites*, bryozoans, gastropods, and oyster shells. This facies type is recorded in the Gebel el Ramliya section. | The texture reflects the water agitation between quiet and moderate in shallow-water subtidal regime of the shoal and above fair-weather wave base. |
| Nummulite packstone (3b) (Fig. 4a, b) | Laminated to thinly bedded and imbrications. The main components are larger and small *Nummulites*, oyster shells, echinoids, iron oxides and extraclasts. It is recorded in the Mokattam and Minqar el Rayan sections. | The facies suggests a warm, moderately to high agitated shallow water up to 5 m water depth in the shoal setting. |
| Aggregate grains grainstone to rudstone (3c)(Fig. 4c) | Greyish white, small fractured, unbedded limestone with a variety of bioturbation. The facies contains lumps, peloids, micritized skeletal grains, foraminifera and algae. It is recorded only in the Gebel el Ramliya section. | Lumps associated with peloids and micritized grains indicate open and restricted shallow platform. This facies type has been deposited in a lee ward shoal and also in an inner lagoon environment. |
| Alveolinid peloidal grainstone (3d) (Fig. 4d) | Yellowish white to yellow, shows planar to cross-laminated structure, contains alveolinid, peloids, small bivalve debris and echinoids spines. It is recorded only in the Gebel el Ramliya section. | This facies has been deposited in a high energy shallow subtidal shoal, just below low tide level, at water depths less than those of the packstone facies. |
| Nummul. grainstone to rudstone (3e) (Fig. 4e, f) | Snow white, shows hard and massive beds, mainly made up of complete and fragmented tests of *Nummulites*. Peloids, quartz grains and shell debris are recorded. Mainly in the Gebel el Ramliya, Mokattam and Minqar el Rayan sections. | It is interpreted as a carbonate shoal deposits above the normal wave base. |
| Nummulite floatstone (4a) (Fig. 4g). | Yellowish white to grey limestone. The main components are nummulite tests, and molluscan debris. Bioturbation and iron traces are common. This facies is recorded in the Qattamiya section. | Large and flat nummulite indicates the lower photic zone. The scarcity of higher-energy structures suggests deeper water compared to the nummulite rudstone. |
| Numm. bryozoans wacke- to floatstone (4b)(Fig. 4h, i) | Greyish bryozoan reefs, appear as a cross to planar parallel lamination. They are dominated by one species *Tremogastriona fourtaui* interfinger with *Nummulites*. This facies is common in Qattamiya and Mokattam sections. | The abundance of the bryozoans reefs indicates a quiet, protected shelf lagoon environment with open circulation below normal wave base. |
| Bioclastic coralline floatstone (5a) (Fig. 4j, k) | Pinkish brown and buff marly limestones, contain abundant large overturned and dissected isolated branching ovoid and elliptical corals (esp. *Goniopora*). It occurs in the Gebel el Ramliya and the Observatory sections. | Isolated reefs, which are ovoid to elliptical indicates back-reef setting. According to (Bruggemann et al., 2004) The prevailing *Goniopora* sp. indicates sheltered and shallow with turbid waters. |
| Foraminiferal coralline rudstone (5b) (Fig. 4l) | Unbedded and cavernous, lens shaped, brown to buff limestone. It contains large amounts of abraded coral fragments (esp. *Goniopora* and *Cladocora*), diverse foraminifera, bivalve debris, echinoids and coralline algae. The facies type forms several meters thick beds throughout the Gebel el Ramliya section. | According to (Nichols, 1999) The abundance of bioclastic coral rudstones indicates reef setting. The presence of abraded fragments of corals with the larger foraminifera indicates some transportation or reworking of these biogenic grains. |
| Bioclastic coralline bafflestone (5c) (Fig. 4m, n) | Brown, buff to grey massive, highly fractured limestones contain large amounts of coral reef debris of uni. and bifurcated colonial branching types, alveolinid and other foraminiferal tests, coralline algae, bivalves shells, echinoid spines and mud clasts. This facies is recorded in the Gebel el Ramliya and Observatory sections. | The abundance of hermatypic corals means shallow, agitated warm water and high nutrient areas. According to (James and Kobluk, 1978), the coral bafflestones initiated on the reef flat in the reef setting. |
| Foraminiferal coralline framestone (5d) (Fig. 4o) | Pale yellow limestone, consists mainly of low diversity, colonial scleractinian corals, green algae, foraminifera, bivalve shells, and peloids. The facies is only recorded in the Gebel el Ramliya section. | According to (Wei Shen et al., 2008) the massive and dense corals framestone indicates reef crest and margins. This facies type is interpreted as reef crest in the reef setting. |

## 3. Lithostratigraphy

According to Said (1990) no overall classification for the Eocene stratigraphy of Egypt - neither lithostratigraphy nor biostratigraphy - is universally accepted. Accordingly, the chronostratigraphy is not fully standardized. The same can be said about the Middle Eocene of Egypt which has been intensively studied for decades. The lithostratigraphy of the Middle Eocene in the studied areas has been dealt with by many authors which classified the Eocene strata into different rock units in the Fayum, Cairo and the North-Eastern Desert, respectively. The rock units are marked by vertical and lateral facies changes controlled predominantly by major eustatic sea-level variations, and minor synsedimentary tectonic activities reflecting different facies types from Fayum in the west to North Eastern Desert in the east (e.g. Strougo, 1985a, 1985b, 2008; Strougo and Boukhary, 1987; Said, 1990; Helal, 1990, 2002; Strougo and Abd-Allah, 1990; Strougo and Azab, 1991; Gingerich, 1992; Abdel-Fattah et al., 2010; and Sallam et al, 2015a,b). These obvious facies changes will facilitate the high resolution sequence stratigraphic correlation between the studied sections.

The different lithostratigraphic classification of the Middle Eocene rocks in the studied sections is summarized in Table 1. In northern Egypt six sections were measured. These sections are represented by two formations in each locality. In the Fayum area, the two distinguished formations from the base to the top are as follows:

a. Wadi el Rayan Formation: It consists mainly of claystone, marl and glauconitic limestone packed with *Nummulites gizehensis* at the lower part, Nummulite – bryozoan limestones and bivalve shells marly limestones in the middle part and chalky limestone with abundant *Nummulites* spp. at the upper part. According to Strougo (2008) the lower and middle parts are equivalent to the Lutetian stage of the Midawra Member (or Formation) and the upper part is equivalent to the lower Bartonian stage of the Sath El Hadid Member (or Formation). The studied part of this formation at Minqar el Rayan section is overlain Muweilih Member (or Formation) and underlain Gehannam Formation.
b. Gehannam Formation: It overlies the Wadi el Rayan Formation and overlain by the upper Eocene Birket Qarun Formation. It consists mainly of alternating beds of yellowish green calcareous claystones and sandstones dominated by whale bones of *Zeuglodon isis.* Depending on the Planktonic foraminifera and calcareous nannofossil (Strougo et al., 2013), the age of this formation is dated to the upper Bartonian stage.

Towards Cairo at the Gebel Mokattam section, two formations have been studied from base to top:

a. Upper Building stone Formation (or Member): It consists of interbedded limestone as well as marly limestones with several nummulite layers in the lower part dominated by *Nummulites*

**Table 3**
Lithofacies associations (LFA) of Middle Eocene in northern Egypt.

| Lithofacies association | | Depositional environment | Sedimentary features | LFT |
|---|---|---|---|---|
| LFA 1: Tidal flat | Landward | lee ward of tidal flat deposits, developed during arid climate, no distinct lamination or bedding with rare shell fragments (Zonneveld et al., 2001). | Mostly silty clay, thin crusts and pockets of halite and gypsum are common, no admixed terrigenous sand is recorded. | 1a |
| | Bay deposits | Low-energy bay-margin characterized by low angle cross-laminated and massive appearances of bleeding as a result of bioturbation (Telford, 1988) | Fissile, gypsiferous, and slightly ferruginous shale and sand, abundant gypsum-filled joints, with very rare wave ripples and low angle cross lamination. | 1b |
| | Seaward | Low-energy intertidal zone which is characterized by small scale cross bedding in sand, burrows are common, fine shell hash present (Sedgwick and Davis, 2003). | Silty clay to mudstone with thin, irregular to lenticular laminae of silt and fine sand, moderately sorted, micaceous; some iron traces are recorded. | 1c |
| LFA 2: Inner shelf | Rest. inner lagoon | Low energy, with detrital content, formed in a quiet water below fair weather wave base (Fwwb). It is separated from the inner lagoon by the local and limited aggregate grains which indicate some transport and reworking. | Poorly sorted and flaser bedding wackestones and grainstones contain miliolids, gastropods, bivalves, dasyclad algae, arenitic and lumps and grapestones and peloids. Micritization and dolomitization are the main diagenitic features. | 2a, 2b, 3c |
| | Inner lagoon | Low energy, shallow water with semi- restricted circulation of marine water below fwwb, dominated by phototrophes and small *Nummulites* (Adabi et al., 2008). | Bioclastic foraminifera wackestones and packstones, poorly sorted, matrix supported and fossiliferous. Micritization, recrystallization and biotic zonation are common. | 2c, 2d, 2e, 3a |
| LFA 3: Shoal deposits | Landward | Carbonate sands commonly redistributed into the lagoons by storms. Occurs over wide areas of the open marine platform. It contains in some parts nummulite grains deposited by short-term high energy events with open circulation (El Ayyat, 2013). | Alveolined and nummulite grainstones to rudstones characterized by imbricated, moderately to well sorted, planar to cross bedded. biozonation is common | 3b, 3c |
| | Seaward | Hard, massive to bedded nummulite layers with oysters with water depth near to the fwwb (Kovacs, 2005). | Nummulite packstones to floatstones encrusted by small oysters or membraniporiform bryozoans. Imbrications and drusy cements are common. | 3d, 3e |
| LFA 4: Outer lagoon & back reef | Leeward | Low energy outer lagoon occurred in rimmed shelves protected from strong wave actions by reefs. Normal marine salinity (Addi, 2015). | Consists mainly of echinoid and bryozoan wackestones and bafflestones, poorly sorted, cross bedded. Aggrading neomorphism is common. | 4a, 4b. |
| | Seaward | Developed on the interior area of a carbonate bank, low energy. Located behind the bank margin reefs (Cabioch et al., 2008). | Consists mainly of poorly sorted coralline floatstones with badly preserved benthics, molluscs and echinoids. | 5a |
| LFA 5: Reef margin or framework | Reef flat | The shallow area developed adjacent to bank margin reefs; interior patch reefs in an open marine (Racki, 1993). | Consists mainly of coralline rudstones and bafflestones with benthics, molluscs, large- sized gastropods and bivalves. Micritization is common. | 5b, 5c |
| | Reef crest | Sharp break in slope at seaward margin or edge of reef flat; flourish in shallow warm waters and high nutrient areas (Blanchon et al., 2002). | Consists mainly of poorly sorted, massive and dense coral framestones with foraminifera and algae. Aggrading neomorphism and micritization are common. | 5d |

*praestriatus* and *Nummulites bullatus.* Above the nummulite beds, there are massive and cross-stratified molluscan beds. Further up in the section, thick bedded argillaceous nummulite echinoid limestones have been recorded, which consist mainly of Nummulites spp. and infaunal burrowing echinoids, such as *Schizaster mokattamensis.* The upper part composed of marly limestone crowded with bivalve shells of *Vulsella* sp. and *Wakulina* sp. The studied Formation overlies the Gizehensis Formation (or Member) and underlies the Giushi Formation (or Member). Depending on the nummulite studies of Boukhary and Kamal (1993), the age of the Upper Building stone is dated to upper Lutetian stage.

b. Giushi Formation (or Member): it overlies the Upper Building stone Formation (or Member) and underlies the Upper Eocene Maadi Formation. The lower part of this formation consists mainly of bioclastic limestone with relics of nummulite tests and shell hash, and is overlain by thick-bedded nummulite bryozoan marly limestone beds. The bryozoan beds are dominated by Tremogastrina fourtaui, while the *Nummulites* bands contain large amounts of *Nummulites discorbinus* and *Nummulites praestriatus.* The upper part is characterized by argillaceous limestones with shell hash and scattered nummulite tests. Depending on the nummulite and bivalve tests studies of Strougo (1985a and 2008), the age of the Giushi dates to the Bartonian stage.

At the north Eastern Desert, three sections have been studied and two formations from the base to the top have been distinguished:

a. Observatory Formation or (Sannor Formation): The Observatory Formation is clearly recorded in the all three studied sections. The base of this formation consists of bioclastic nummulitic limestone, followed upward by bryozoan limestone at the Qattamiya section and foraminiferal coralline marly limestone in the Observatory and Gebel el Ramliya sections. The upper part of this formation consists of foraminiferal dolomitic limestone with the remains of miliolids and bivalve shells at the Qattamiya section, nummulite limestone and shell hash at the Observatory section and coral debris, echinoids, gastropods and large foraminiferas at the Gebel el Ramliya section. The Observatory Formation overlies the Gizehensis Formation (or Member) and underlies the Qurn Formation. Based on Said (1990), Shahin et al. (2007) and Strougo (2008) the age of the observatory Formation in the studied sections is Late Lutetian – Early Bartonian stage.
b. Qurn Formation: It overlies the observatory Formation and overlain by the Upper Eocene Wadi Hof or Maadi formations. Based on foraminiferal assemblages, Strougo and Boukhary (1987) and Sallam et al. (2015b) suggested a Bartonian stage to this formation. The lower part of it starts with thick bedded, bioclastic limestone containing *Nummulites*, echinoid spines and bivalve shells at both of Qattamiya and Observatory sections while at the Gebel el Ramliya section the lower part is characterized by cross-bedded bioclastic limestones dominated by large foraminiferas, echinoids, bryozoans as well as bivalve shells and peloids. The middle part of this formation at the Qattamiya section consists of chalky bioclastic bryozoan limestone with an abundance of bryozoans, *Nummulites* spp., serpulids and echinoids. Instead of the bryozoan beds, bioclastic corals beds are characterise the middle part of this formation at the Observatory and the Gebel el Ramliya sections. The upper part of this formation consists of limestone beds with *Nummulites* spp., bivalve shells dominated by oyster shells, as well as gastropods at the Qattamiya and the Observatory sections, while at the Gebel el Ramliya section small oval to circular patches of dendroid corals exist which are intercalated with bioclastic limestones.

## 4. Methodology

Six Middle Eocene stratigraphic sections were described, measured and examined in the area bounded by Wadi el Hitan in the Western Desert and Wadi el Ramliya in the Eastern Desert. These are from the west to the east respectively: The Wadi el Hitan section (29° 14′ 49″ N, 30° 07′ 13″ E), The Minqar el Rayan section (29° 07′ 09″ N, 30° 20′ 23″ E), the Mokattam section (31° 17′ 15″ N, 30° 00′ 37″ E), the Qattamiya section (29° 58′ 12″ N, 31° 24′ 24″ E), the Observatory section (29° 56′ 03″ N, 31° 49′ 38″ E) and the Gebel el Ramliya section (29° 45′ 01″ N, 32° 00′ 33″ E). These sections were described with respect to their texture, fossil content, grain type and size, sorting, bedding style, and primary sedimentary structures of the rocks, facies and interpretation of depositional setting and the appearance according to the lithofacies association code (Fig. 2). Six hundred and twenty five rock samples were prepared and examined from the studied sections. Two hundred and twenty thin-sections were prepared and examined under polarizing microscope to integrate lithological, paleontological and diagenetic data for facies characterization, and to construct conceptual 3-D depositional/lithofacies association model for the investigated Middle Eocene outcrop sections.

## 5. Results and discussions

### 5.1. Facies analysis and interpretation

Nineteen lithofacies types (LFT) were distinguished in the Middle Eocene rocks in the study area (Table 2). At all the studied sections, the lower part of the Lutetian (early Middle Eocene) is massive and dominated by dolomitic limestone embracing several nummulite banks, and other fossil remains. The upper part is dominated by coralline algal limestones and marly limestones in the Gebel Ramliya and Observatory sections, echinoid limestones at the Mokattam section, and intercalations of limestone and clastic sediments in the Minqar el Rayan section.

The Bartonian (late Middle Eocene) sections of the Gebel Ramliya and Observatory sections are also dominated by coralline and marly limestone, including corals, bivalves, gastropods, echinoids and calcareous algae. While in the Qattamiya and the Mokattam sections, thin bedded bryozoan limestone beds are recorded, with small nummulite and gastropods, capped by dolomitic and oyster shell bands. In the Minqar el Rayan section, the Bartonian rocks are represented by thick-bedded limestone with *Nummulites* spp., bivalve shells and bryozoan bands at base, followed upward by clastic sediments.

### 5.2. Lithofacies associations (LFA) and depositional model

Facies types were grouped into five lithofacies associations (LFA) that are related to depositional environments. These depositional environments are tidal flat, inner lagoon, shoal deposits, outer lagoon and back reefs and reef framework located on the shallow carbonate platform. The microfacies types, facies associations, as well as depositional environments of the studied Eocene rocks are outlined in Table 3, and illustrated in (Figs. 3 and 4). Based on these data, a model is given for the studied Middle Eocene rocks at the studied area (Fig. 5).

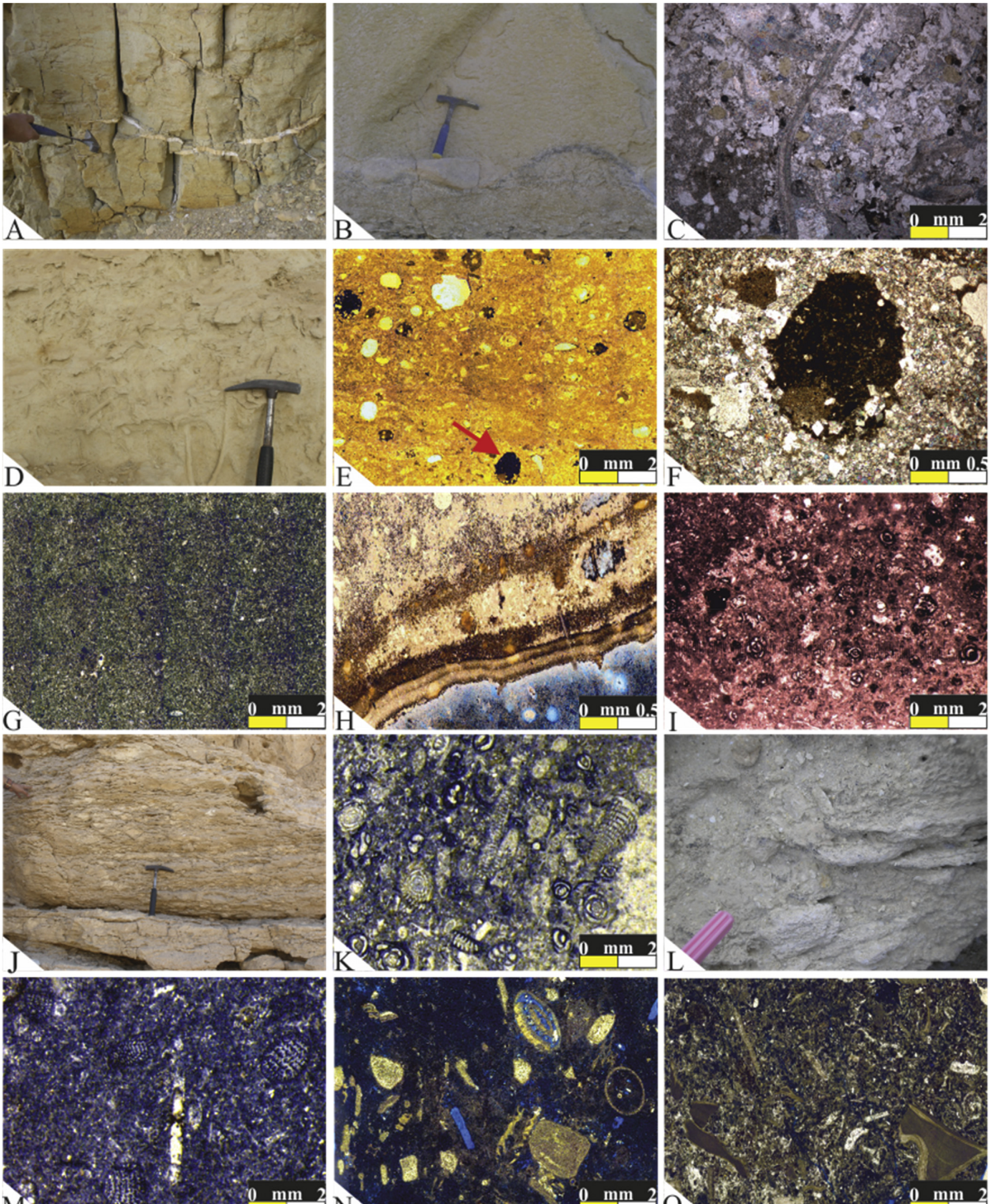


**Fig. 3.** **A**. Fractured claystone with gypsiferous bands. S1, Minqar el Rayan Section. **B**. Well preserved whale skeleton in a sandstone bed, S3, Wadi el Hitan section. **C**. Calcareous quartz arenite, with bivalve debris and small micrite grains. S3, Wadi el Hitan section. **D**. Bioturbated sandstone with intensively burrows. S3, Wadi el Hitan section. **E**. Bioclastic dolostone shows mud and lithic clasts in dolomitic texture. G. el Ramliya section. **F**. Magnification of the mud clast (arrow in e) contains euhedral to subhedral dolomite crystals embedded in a dolomite texture, G. Ramliya section. **G**. Lim-mudstone shows scattered skeletal grains. S2, Minqar el Rayan section. **H**. Stromatolite algal wackestone. S1, G. Ramliya

### 5.3. Sequence stratigraphy

The sedimentary sequences might be the result of eustatic sea-level fluctuations and/or tectonic movements (Catuneanu et al., 2009) The common sedimentary cycles recognized in the study area were developed in response to relative sea level change, ranging from reef framework to tidal flat environments. In this study, the lithofacies types are stacked into five facies cycles. The terminology to describe the facies cycles was adopted from Kerans and Tinker (1997). Accordingly, cycles (fifth-order) are stacked to form cycle sets (fourth-order) that are arranged in sequences (third-order), which form the overall Middle Eocene rocks in the area under study. The described cycles, cycle sets and sequences were subdivided into transgressive and regressive parts. They are separated by turnarounds, i.e. zones of maximum and minimum accommodation (Cross and Lessenger, 1998).

#### 5.3.1. Small-scale cycles (cycles)

Facies types are stacked to fifth-order transgressive-regressive cycles, usually range from several decimetres to a few metres (Embry, 1993). These cycles exemplify the finest scale of cyclicity within the studied sections. Small-scale cycles can be subdivided into a transgressive and regressive hemicycle. Similar to the hierarchical subdivision of facies associations and facies types, six small-scale cycles are recognized in the studied rocks and are summarized in (Table 4).

#### 5.3.2. Medium-scale cycles (cycle sets)

Stacking of 3–6 cycles constitute transgressive-regressive cycle sets, ranging from 12 to 25 m in thickness. In the present work, the studied sections are subdivided into 3 depositional sequences (S1, S2 and S3), each of these sequence includes 3 to 4 cycle sets (Table 5). Sequence 1 includes CS 1.1, CS 1.2 and CS 1.3. Sequence 2 includes CS 2.1, CS 2.2 and CS 2.3. Seuence 3 includes CS 3.1, 3.2 and 3.3.

#### 5.3.3. Large-scale cycles (sequences)

##### 5.3.3.1. Sequences descriptions

A. **Sequence 1:** S1 ranges in thickness from 35 to 45 m, and forms the lower part of the Observatory Formation at the Gebel el Ramliya, Observatory and Qattamiya sections, the Upper Building Stone Member of the Mokattam section, and the lower part of the Wadi el Rayan Formation at the Minqar el Rayan section. The base of this sequence represents the boundary between the Gizehensis Member and the Observatory or the Upper Building Stone Member at Gebel el Ramliya, Observatory, Qattamiya and Mokattam sections or in the lower part in the Midawara Member at Minqar el Rayan section. From west to east, i.e. from landward (proximal) to seaward (distal), the lower part begins with moderately hard and thin-bedded *Nummulites* packstone, packed with *Nummulites gizehenesis* which alternate with claystone and marly limestone layers at the Minqar el Rayan section. At the Mokattam, the Qattamiya, and the observatory sections, the beginning of the lower part is characterized by interbedded bioclastic wacke-to mudstone as well as marly limestone with several *Nummulites* layers in the lower part dominated by *Nummulites praestriatus* and *Nummulites bullatus*. The accumulation of *Nummulites* spp. progressively increases upwards and is mainly composed of light brown-grey *Nummulites* wacke to-packstone. Occasionally, some mudstone intervals can be observed. Besides the *Nummulites* spp., also common are *Operculina* sp., *Discocyclina* sp., ostracods and rotaliids. At the Gebel el Ramliya, the section also starts with *Nummulites* grain-to rudstone beds. Above the basal parts of S1, we find alternations of *Nummulites* echinoid wackestones and thin nummulite bivalve wacke-to packstone at the Minqar el Rayan, Mokattam, Qattamiya and Observatory sections. The echinoid beds are dominated by infaunal echinoid burrows, such as *Schizaster mokattamensis, Fibularia* sp. and *Eupatagus* and the bivalve shells at the Qattamiya section show vesicular and foliated microstructures (*Fimbria* sp.), echinoids (*Echinocyamus* sp. and *Echinolampas* sp.) and large foraminifera. At the Gebel el Ramliya section the nummulite beds are followed by a coral community with a relatively low diversity, consisting of accumulations of broken, irregularly arranged small fragments of branching corals such as *Gonipora* sp. The upper part at the Minqar el Rayan and Mokattam sections consists of molluscan wackestones dominated by bivalve casts and gastropods. At Qattamiya, Observatory and the Gebel el Ramliya, the upper part is dominated by bioclastic wacke-to floatstone consisting of foraminifera and shell accumulations, all of which are intercalated with thin dolostone layers. The top of this sequence is marked by a sharp contact of ferruginous and gypsiferous claystone in the Minqar el Rayan, Mokattam, and Qattamiya sections, dolomitized lime mudstone at the Observatory section and algal wackestone lamina at the Gebel el Ramliya section.

B. **Sequence 2:** S2 ranges in thickness between 40 and 70 m. It forms the Late Lutetian and the Early Bartonian of the upper part of the Observatory Formation or Sannor Formation in the Gebel el Ramliya, Observatory and Qattamiya sections, the lower part of the Giushi Formation in the Mokattam section and the upper part of the Wadi el Rayan Formation at the Minqar el Rayan section. Moving along S2 from the west to the east, it is observed that the base of this sequence is dominated by lagoonal lithofacies of molluscan wacke-to packstone, packed with bivalve shells and gastropods with relics of *Nummulites* tests in the Minqar el Rayan and Mokattam sections. The same is observed in the Qattamiya section but some mudstone and marlstone beds are intercalated. Above these bases, there is nummulite bryozoan wacke-to floatstone dominated by *Tremogastrina fourtaui* and small clypeasteroid echinoids intercalated with thin beds of sandy lime-to marlstone. The same situation is also in the Qattamiya section with further additional species of the bryozoan such as *Membranipora* sp. erect rigid forms of *Steiginoporella* sp. and erect flexible forms of *Nellia* sp. The Observatory and the Gebel el Ramliya sections show lateral changes from a lagoonal lithofacies to a reef lithofacies and exhibited bioclastic coralline algal floatstones containing mainly hemispherical to spherical branching corals bored by bivalves and encrusted by coralline red algae and serpulids. Most of the coral branches are broken which may be due to agitated wave action. These floatstones are overlain by coral boundstone, with an increasing amount of reefal debris and branching corals such as *Astroconia* sp., *Stylophora* sp., *Dendracis* sp. and *Madrepora* sp. The upper part of S2 at all the sections consists mainly of bivalve shells packed with *Vulsella* sp. and *Wakulina* sp. and

section **I**. Foraminiferal miliolid wackestone, shows miliolid tests in micrite matrix. Few inclusions of detrital grains are appeared. S3, G. Ramliya section. **J**. Flaser bedding, S2, Gebel el Ramliya section. **K**. Foraminiferal wackestone contains high amount of foraminiferal shells. S2, G. Ramliya section. **L**. Bioclastic wackestones contain small nummulite and gastropods. S3, Qattamiya section. **M**. Thin section photograph of a sandy bioclastic nummulite wackestone, S3, Qattamiya section. **N**. Echinoid fragments of plates and annelid tubes filled with micrite. S2, Gebel el Ramliya section. **O**. oyster shells wacke-to packstone on the top of the Qattamiya section.

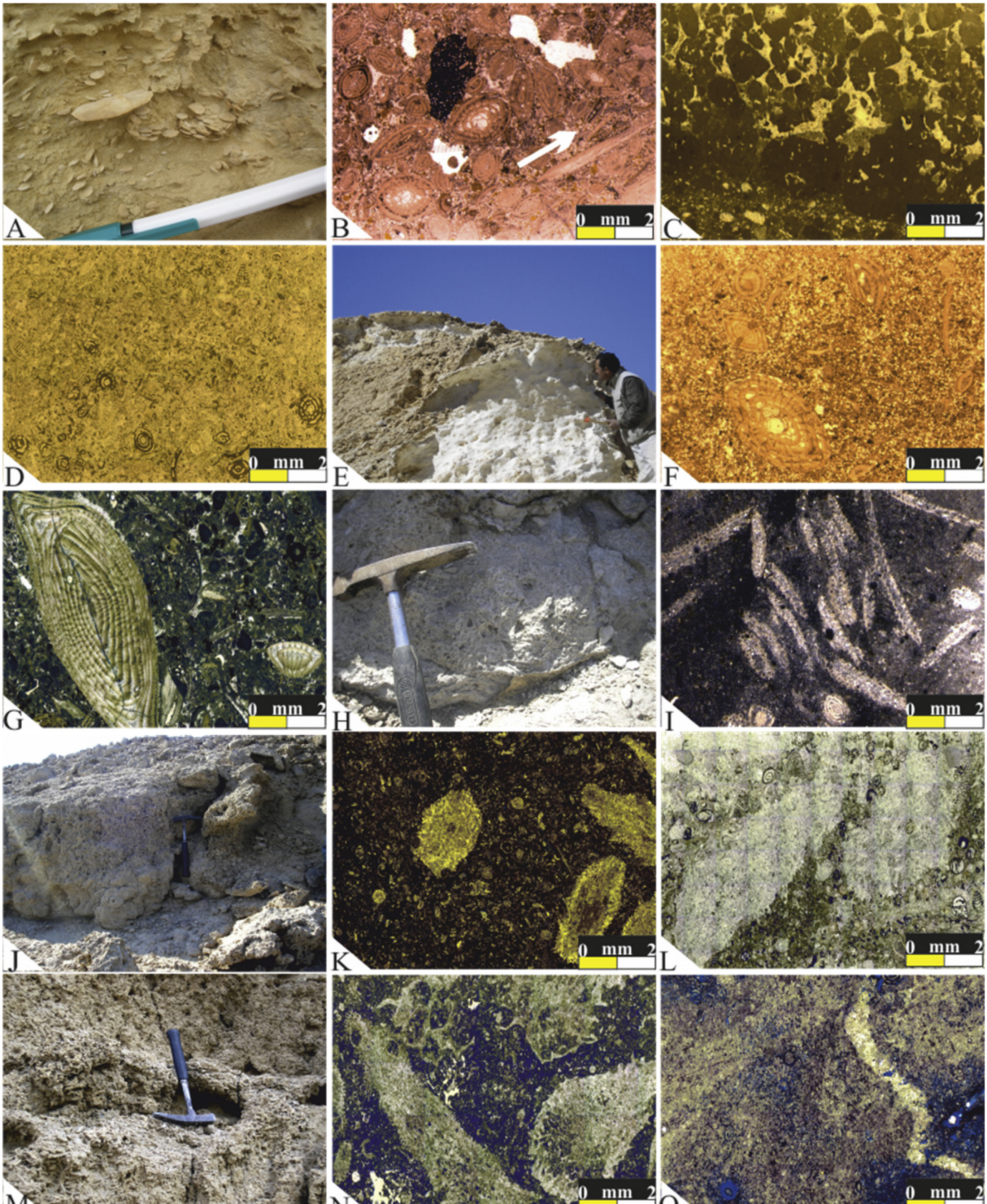


**Fig. 4. A**. Nummulite bank consisting of different sizes of *Nummulites*. Notice the imbrications of *Nummulites* tests. S1, Minqr el Rayan section. **B**. Nummulite packstone shows radial hyaline and perforated tests, consisting predominantly of *Nummulites*. Note imbrication of grains (arrow). S2, Minqr el Rayan section. **C**. Micritized aggregate grains (lumps) exhibiting the characteristic lobate outline. The composite grains consist predominantly of peloids and some bioclasts bound together by microcrystalline calcite. Most grains have rims of thin early-marine cement. S2, Gebel el Ramliya section. **D**. Micritized alveolinid grains imbedded in pelodial grainstone. S3, G. el Ramliya section. **E**. Chalky limestone

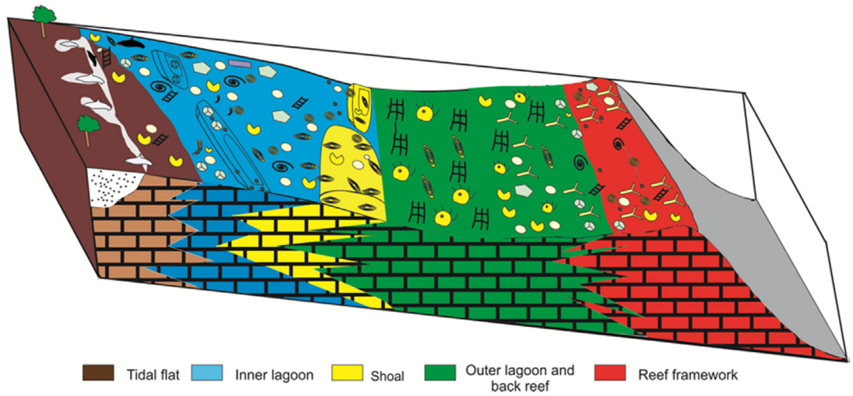


**Fig. 5.** Conceptual 3D depositional/lithofacies association model for the investigated Middle Eocene outcrop sections.

foraminiferal wake-to mudstone beds containing *Nummulites* and in the Gebel el Ramliya section, adding to the nummulite beds, some of *Dictyoconus egyptiensis*, *Idalina* sp., *Somalin*a sp. and *Rhabdorites* sp. dominate. The uppermost part of these sections, except the Gebel el Ramliya, consists mainly of poorly fossiliferous hardground dolo-mudstone exhibiting a sharp upper contact. In the Gebel el Ramliya section, S2 is capped by a 50 cm thick, ferruginous burrowed mudstone, which is partly dolomitic and exhibits gradational contact.

C. **Sequence 3:** S3 ranges in thickness from 25 to 55 m and is composed of three cycle sets and ten cycles, which characterise the Upper Bartonian Qurn Formation in the Gebel el Ramliya, Observatory and Qattamiya sections, the upper part of the Giushi Formation in the Mokattam section, and the Gehannam Formation in the Wadi el Hitan Section. The last bed of this sequence represents the sequence boundary between the Middle Eocene (Bartonian) and the Upper Eocene (Priabonian) rocks. Just like the previous sequences, from the west to the east, the lower part of S3 at the Western Desert is represented at the Wadi el Hitan section and consists of clastic rocks of bioturbated sandstone that is highly burrowed by gastropods and is rich in fish scales, shark teeth, and abundant whale bones. In the other sections, the lower part consists mainly of cross-bedded bioclastic wacke-to packstone, which is moderately sorted and rich in fossils, such as foraminifera, echinoid plates and spines. Further up in the sequence in the Mokattam and Qatamiya sections is some bioclastic bryozoan wackestone with abundant bryozoans, *Nummulites* spp., serpulids and echinoids but in the Observatory and Gebel el Ramliya sections, the basal part is overlain by a thick bed of bioclastic coralline algal boundstone, and is dominated by overturned and broken branched and meandroid corals. Large foraminifera (alveolinid), coralline algae, echinoids and bivalve debris fill the cavities between coral branches. The upper part of the Wadi el Hitan section consists of weakly bioturbated sandy shales and sandy siltstones characterized by low-angle cross-lamination. Fissile, gypsiferous and slightly ferruginous shales are abundant and gypsum fills many joints. In the Mokattam, Qattamiya and Observatory sections the upper part consists of bioclastic foraminiferal wackestone beds, which contain *Nummulites* spp., micritized miliolid and bivalve shells dominated by oyster as well as gastropod shells. The upper part of the Gebel el Ramliya section consists of small oval to circular patches of bafflestone as well as floatstone formed by corals that are intercalated with bioclastic foraminiferal grainstone beds. The uppermost part of Sequence 3 is characterized by, at Wadi el Hitan, the presence of root casts and an assemblage of brackish marine invertebrates, in the Mokattam and the Qattamiya sections, a sandy marlstone layer that contains scattered quartz grains and iron oxides, and at the Observatory and the Gebel el Ramliya sections, a poorly fossiliferous mudstone containing relics of miliolids and other smaller benthic foraminifera.

#### *5.3.3.2. Sequences interpretations*

A. **Sequence 1:** The nummulite beds in the lower parts of the sequence 1 indicate a shoal to inner lagoon related facies (Rasser et al., 2005) and could be interpreted as an initial transgressive hemi-sequence. During the sea level rise, the change from proximal nummulite beds to distal echinoids and coral beds occurred and the maximum flooding interval is represented on a top of the echinoid and reef beds. The upper part, which is interpreted as a regressive hemi-sequence, consists of muddy facies and indicates a depositional shift toward the inner lagoonal setting (Maanan et al., 2004) during a sea-level fall. The sharp contact on the top of this sequence in all sections represents the sequence boundary between Sequence 1 and Sequence 2.

B. **Sequence 2:** The molluscan beds as well as coral floatstones in the lower parts of sequence 2 indicate an inner lagoon (Castro et al., 2008) or back reef related facies (Pomar and Hallock, 2007) and could be interpreted as an initial transgressive hemi-sequence. The change when the sea level rose, from proximal inner lagoon beds, or back reefs in the Eastern Desert sections, to distal outer lagoon bryozoan beds or reef framework beds, can be interpreted as a maximum flooding zone. The upper part of this sequence represents a regressive part; it consists

represents the MFS at the top of the Minqar el Rayan section. **F.** Sandy bioclastic nummulite grainstone/rudstone. The matrix consists of angular, fine sand sized quartz grains (white). S3, Qattamiya section. **G.** Bioclastic nummulite floatstone, notice the micrite grains, S3, Qattamiya section. **H.** Bryozoan reef, S2, Mokattam section. **I.** Nummulite bryozoan wacke-to floatstone. S2, Mokattam section. **J.** Bioclastic coralline floatstone, represents the MFS of the S2, Observatory section. **K. C**oral fragments embedded in micrite matrix contains foraminiferal tests especially miliolids. S3, G. el Ramliya section. **L.** Foraminiferal coral fragments rudstone. S2, G. el Ramliya section. **M.** Numerous broken branching corals at the transgressive part of the S3, G. el Ramliya section. **N.** Resistant coralline bafflestone S3, G. el Ramliya section. **O.** coral reef framestone with massive and branching corals. Chambers of coral are filled with an isopacheous crust of early marine acicular cement. S3, G. Ramliya section.

**Table 4**
Small scale cycle types.

| Small-scale cycle types | Thickness | Distribution | Description | Interpretation |
|---|---|---|---|---|
| Reef core (Fig. 6) | 4–6 m | Transgressive parts of S2 and S3 at the Gebel el Ramliya section and Observatory sections | The lower part is several decimeters thick, starts with thick bedded bafflestones with small dendroid coral species such as *Goniopora* sp. (LFT 5c). The coral bafflestone is overlain by up to 1.5 m thick coral boundstones with an increasing amount of reef debris, and contains uni-, bi- and tri-furcated branching corals, especially *Madrepora* sp., *Stylophora* sp., *Dendracis* sp. and *Astroconia* sp. (LFT 5d). The whole boundstone is neomorphically altered and no internal structures are preserved. The cycle is capped by thinner bedded, foraminiferal or peloidal grainstone, contains a specific biota, such as benthic foraminifera especially alveolinid and green algae (LFT 3d). | Coral beds in the lower part of this cycle type represent a moderate energy distal reef flat related facies type Benisek et al. (2009), forming a transgressive hemi-cycle. The interval with the highest amount of coral debris, and the high diversity of corals is interpreted as a maximum flooding zone (MFZ). The regressive hemi-cycle is interpreted as the progradation of a more proximal shoal facies types over the coral reef facies. |
| Back-reef and Outer lagoon (Figs. 7 and 8) | 3–6 m | Transgressive and regressive parts of all sections except at Wadi El Hitan. | The basal unit is several decimeters thick, starts with miliolid wackestone (LFT 2b) which gradually changes upwards to bioclastic coralline floatstone in the Gebel el Ramliya and Observatory sections (LFT 5a), composed of coral fragments which are of the head-like or branching type. The matrix is mainly composed of skeletal fragments with some coated grains. Or bryozoan beds in the other sections (LFT 4b). The upper part of this cycle type consists of foraminiferal wackestone which is dominated by micritized benthic foraminifera, especially miliolids and orbitiolids (LFT 2c). | The predominance of mud-rich lithology with miliolids, as well as the presence of a low-diversity foraminiferal association in the lower part of this cycle type indicates a shallow restricted lagoonal environment with low energy (Vaziri-Moghaddam et al., 2006) which forms the transgressive hemi-cycle. The overlying coralline floatstone or bryozoan beds, deposited under moderate to low energy condition are interpreted as a MFZ, while the upper part is interpreted as a low energy inner lagoon related facies forming a regressive hemi-cycle. |
| Shoal (Fig. 9) | 4–6 m | Transgressive and regressive parts of the Qattamiya, Mokattam and Minqar el Rayan sections. | The base of this cycle is represented by dm-thick bioclastic packstones with local wackestones. The bioclasts are dominated by worn thinly bedded bivalve shells, red algae, and forams (LFT 3a). The skeletal remains are packed in granular calcite with some partially recrystallized lime mud matrix. Upwards, this unit is followed by well sorted and cross-bedded nummulite packstone to grainstone, with a thickness of 2 m and more. The facies is dominated by *Nummulites* spp. Other associated microfauna such as echinoid spines and bivalve shells are also represented (LFT 3b). The upper part consists of brownish yellow, thin interbedded argillaceous mudstone and marl, with sparse fauna of ostracods and shell hash. (LFT 2a). | Bioclastic packstone to wackestone at the base of this cycle type indicates a low energy inner lagoonal facies association and represents the transgressive hemi-cycle. The energy increases around the top of the transgressive hemi-cycle, with well-sorted and cross-bedded nummulite packstone forming a nummulite bank (Aigner, 1985), and is interpreted as a maximum flooding zone. The regressive hemi-cycle may be represented by the transition from the shoal to a more proximal tidal flat condition. |
| Inner-lagoon (Fig. 10) | 2–4 m | Transgressive and regressive parts of all sections except of Wadi El Hitan | The basal part is several decimeters thick, begins with dolomitic mudstone to wackestone with relics of miliolids, *Nummulites* sp. and bivalve shells (LFT 2d). Overlaying the basal part is a 0.5–1 m thick bioclastic wacke- to packstone bed (LFT 2c). This cycle type is capped by thin laminated and highly porous argillaceous wackestone to mudstone, ranging in thickness from 0.5 to 1.5 m, containing intraclasts, scattered detrital quartz grains as well as fenestral fabric (LFT 1c). | Dolo-mudstone at the base of the cycle type indicates low energy tidal flat Nakazawa and Ueno (2004) and represents a transgressive hemi-cycle. The MFZ is defined at intervals with a maximum percentage of open marine components and fossils. The regressive hemi-cycle consists of tidal flat mudstone, interpreted as a progradation of the tidal flat facies that caused by a sea level fall. |
| Tidal-flat (Fig. 11) | 4–6 m | Transgressive parts of the Minqar el Rayan section | The basal part of this cycle, up to 2.5 m thick, consists mainly of siltstone and overlay by fine sandstone with shell hash (LFT 1b). The vertical thickness of the upper part ranges in thickness from 2 to 2.5 m and consists of greenish silty claystones with rare shell fragments. No distinct lamination or bedding is detected (LFT 1a). | Siltstones and the fine sandstones in the lower part of this cycle indicate seaward tidal flat and represent a transgressive hemi-cycle. The MFZ is defined at the top of the sandstone layers. The regressive hemi-cycle is represented by the transition from the seaward to leeward tidal flat. |

of muddy facies and indicates a depositional shift again towards an inner lagoon setting. The ferruginous dolo-mudstone lamina on the top of this sequence is associated with short term exposure and it marks the sequence boundary between S2 and S3.

C. **Sequence 3:** The lower part of this sequence is interpreted as an inner lagoonal related facies (Fierstine and Gingerich, 2009, Sadeghi et al., 2011), which was deposited under low-energy conditions and represents a transgressive hemi-sequence. During subsequent sea level rise, more distal outer lagoon and reef framework at the Observatory and Gebel el Ramliya related facies types retrograded over the inner lagoonal beds and the maximum flooding interval is interpreted at these beds. The relative fall in sea level is marked by the transition from the distal reef or outer lagoon related facies to the proximal inner lagoonal and tidal flat environment in the upper part of the sequence. The upper most lamina that caps the sequence indicates a more proximal tidal flat related facies and represents the upper sequence boundary.

### 5.4. Sequence stratigraphic discussions and correlations

Sequences can be the result of eustatic sea-level variations and/or tectonic movements at diverse temporal and spatial scales (Aghaei et al., 2013). It can also be created by a variation of processes (Brunet et al., 2009), which will have an effect on the architecture of the stratigraphic record (e.g., Fursich et al., 2003; Catuneanu et al., 2009). The common cycles in most units in the studied sections indicate sedimentary responses to relative sea level change, ranging from reef framework to tidal flat environments. Based on their relative position with respect to other

**Table 5**
Medium scale cycle types.

| Cycle sets | Thickness | Distribution | Description | Interpretation |
|---|---|---|---|---|
| Reef to Back-reef (Fig. 12) | 25 m of 4–6 cycles | CS1.2, 2.1, 2.2, 2.3, 3.2 & 3.3 at the Gebel el Ramliya section and CS 2.3 & 3.2 at the Observatory section | The basal part, up to 2 m thick, consists of bioclastic wackestone. The facies is dominated by benthic micritized foraminifera (miliolids and textulariids) and peloid grains embedded in a neomorphised micritic matrix. Overlying the basal part there are 8–16 m thick of bedded and cavernous bioclastic coralline boundstones and rudstones. The corals consist of massive and branching types. The upper part, some 5–10 m thick, is composed of bioclastic coralline floatstones dominated by abraded coral clasts, echinoid fragments and gastropods. This cycle set is capped by erosional sharp contact of algal conglomeratic wacke- to bindstones in the Gebel el Ramliya and poorly fossiliferous and ferruginous dolo mudstone in the Observatory section. | The wackestone in the lower part is interpreted as an initial transgression. The continuous rise in sea level led to the deposition of distal and high energy bioclastic coralline boundstones and rudstones indicating a reef facies, and is interpreted as a maximum flooding zone. The upper part consists of muddy facies which exhibits a depositional shift toward back reef setting during the fall of sea-level. The sharp contact on the top of this cycle set suggests a low accommodation tidal flat environment and a sequence boundary. |
| Back-reef or outer lagoon to Inner-lagoon (Figs. 12 and 13) | 10–16 m of 4–5 cycles | CS 1.3, 2.4 & 3.1 at the G. Ramliya, CS 1.2, 1.3, 2.1, 2.4, 3.1 & 3.3 on the Observatory, CS 1.2, 2.2 & 2.3 in the Qattamiya, CS 1.2, 1.3, 2.1, 2.2 & 2.3 in the Mokattam and 1.2, 2.2 & 2.3 in the Minqar el Rayan | The basal part of this cycle set ranges in thickness from 2 to 3 m and consists of thick bedded and massive bioclastic pack- and wackestone. It is dominated by *Nummulites*, orbitiolites, miliolids and bivalve shells as *Vulsella* sp. The basal part is overlain in some cycle sets by 6–8 m of floatstone beds, intercalated with bioclastic foraminiferal wackestones associated with small patches of corals, and in other cycle sets is overlain by nummulite bryozoan wacke- to floatstones intercalated with thin marl laminae. The upper part is up to 6 m thick, consists mainly of bioclastic dolo wacke- to mudstone including miliolids, *Dictyoconus*, bivalvian shells and dasycladacean algae. The cycle set is capped by thin bedded marl- to claystones with a sharp erosional contact. | The pack- to wackestones in the basal part is interpreted as an initial transgression within this cycle set. During sea level rise, a back reef or an outer lagoon related facies types are interpreted as retrograding over the inner lagoon deposits and represent a maximum flooding zone. The regressive hemi-cycle is interpreted to be marked by the transition from the distal outer lagoon to the proximal inner lagoon in the upper part. The marl- to claystone bed on the top of this cycle set indicates more proximal tidal flat environments. |
| Shoal to Inner-lagoon (Figs. 12 and 13) | 12–20 m of 5 small-scale cycles | CS 1.1 at the Gebel el Ramliya, CS 1.1 & 2.4 at the Minqar el Rayan section | The lower part of this cycle set is ca. 12 m thick consists of massive nummulite packstones, dominated by complete and fragmented tests of *Nummulites*, and grades upwards to cross bedded nummulite grain- to rudstones. The upper part of this cycle set, up to 5 m thick, consists of bioclastic wackestones, and contains the large amounts of shell hash and ostracods. The cycle set is capped by a decimeter thick, grey to yellowish brown, highly burrowed argillaceous lime mudstones to wackestones. | The lower part indicates distal shoal facies deposited under high energy conditions and represents a transgressive hemi-cycle set. The upper part indicates a transition from a distal high- energy shoal facies to a proximal low energy inner lagoonal facies and represents a regressive hemi-cycle. The top of this cycle set exhibits ferrugination and represents the sequence boundary. |
| Inner lagoon to tidal flat (Figs. 12 and 13) | 10–14 m of 3–5 small scale cycles | CS 1.1 & 2.4 in the Observatory, CS 1.1, 1.3, CS 2.1 and CS 3.3 in the Qattamiya and CS 1.1, 2.4, 3.1, 3.2 & 3.3 in the Mokattam | This cycle set type is identified in the lower part of this cycle set ranges from 6 to 8 m in thickness and consists mainly of bioclastic nummulite wacke- to packstones intercalated with thin mudstone and dolostone layers. Bioclasts are represented by bivalve shells, gastropods (especially *Turritella* sp.) and large forams as *Orbitolites* sp., and *Dictyoconus* sp. The upper part is 4–6 m thick, consists of fossiliferous argillaceous fenestral wackestones interbedded with marl and mudstones. The uppermost bed of this cycle set shows a sharp erosional contact documented by the presence of a burrowed on the top. | The lower part is interpreted as a distal inner lagoon and forms a transgressive hemi-cycle set. The upper part of this cycle set exhibits a shift from inner lagoon to proximal tidal flat forming a regressive hemi-cycle. The sequence boundary is placed on top of this cycle set. The upper sharp contact (burrowed hard ground marlstone) might be associated with short term exposure. |

environments, facies and facies associations within the studied sequences are as follows: sequence-stratigraphic boundaries (SB) are mainly located within tidal flat facies. Boundaries between S1 and S2 and the overlying S3 are of SB1 type, while the boundary between S2 and S3 is gradational and nonerosional (SB2 type). The lowstand System tracts (LST) were not observed within the studied successions but may be represented further to the east. The maximum flooding surfaces (MFS) are mostly located within coral bufflestone and foraminiferal and nummulitic pack-to grainstone.

The interpretation of the observed relative sea level changes in stratigraphic sequences sometimes considers tectonic versus eustatic control (Issawi, 2002, 2005; Osman, 2003; Issawi et al., 2009 and Sallam et al., 2015a,b). The sequence boundary between Lutetian and underlainYpersian or Palaeocene (not covered in this paper) may be regionally observed, and it is clearly related to folding and deformation (e.g. Syrian arc system, rising of the Red Sea Hills, volcanic activity, Lutetian Pyrenean– Atlasic event: the collision of Africa and Europe plates, etc., see for example, Selim

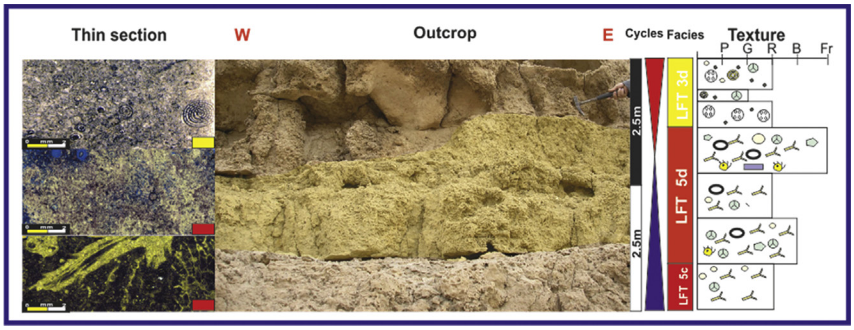


**Fig. 6.** Reef framework cycle type (Gebel el Ramliya section).

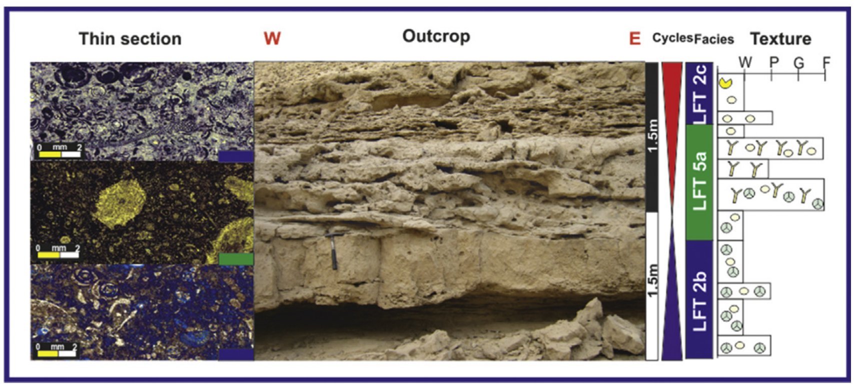


**Fig. 7.** Back reef cycle type (Gebel el Ramliya section).

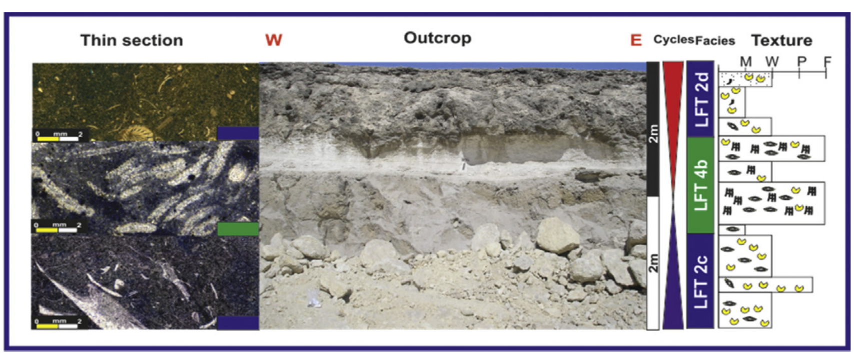


**Fig. 8.** outer lagoon cycle type (Mokattam section).

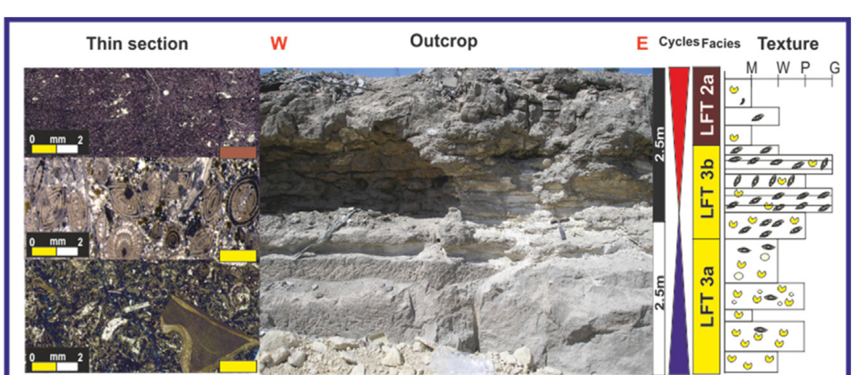


**Fig. 9.** shoal cycle type (Qattamiya section).

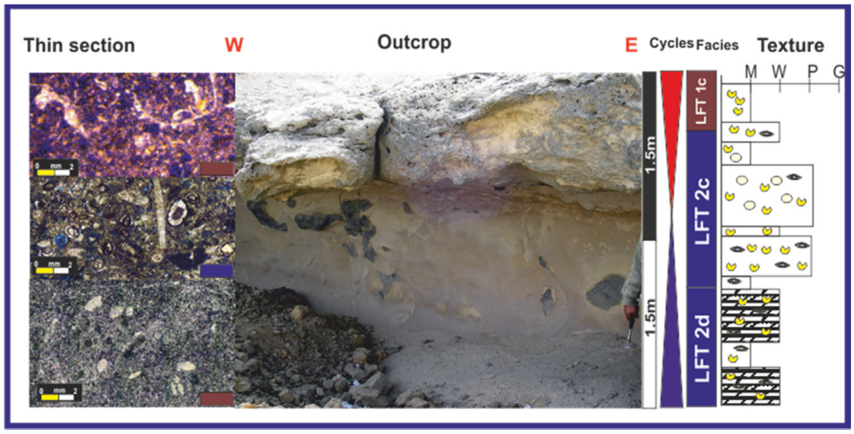


**Fig. 10.** Inner lagoon cycle type (Qattamiya section).

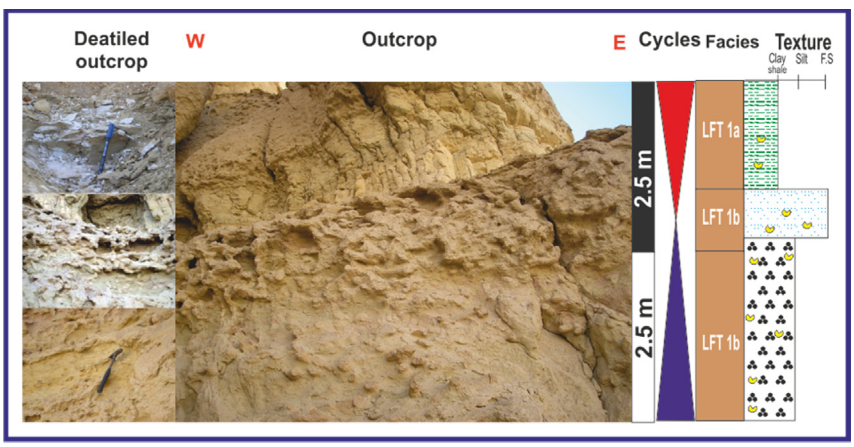


**Fig. 11.** Tidal flat cycle type (Minqar el Rayan section).

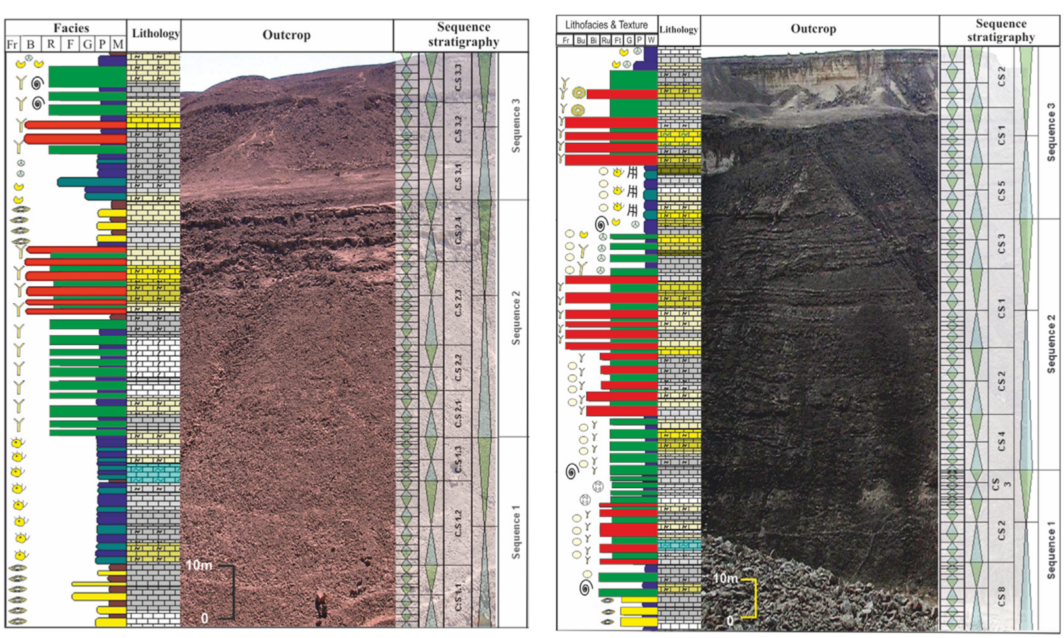


**Fig. 12.** Facies log and interpreted small-, medium- and large-scale cycles of the Gebel el Ramliya section on the right and the Observatory section on the left.

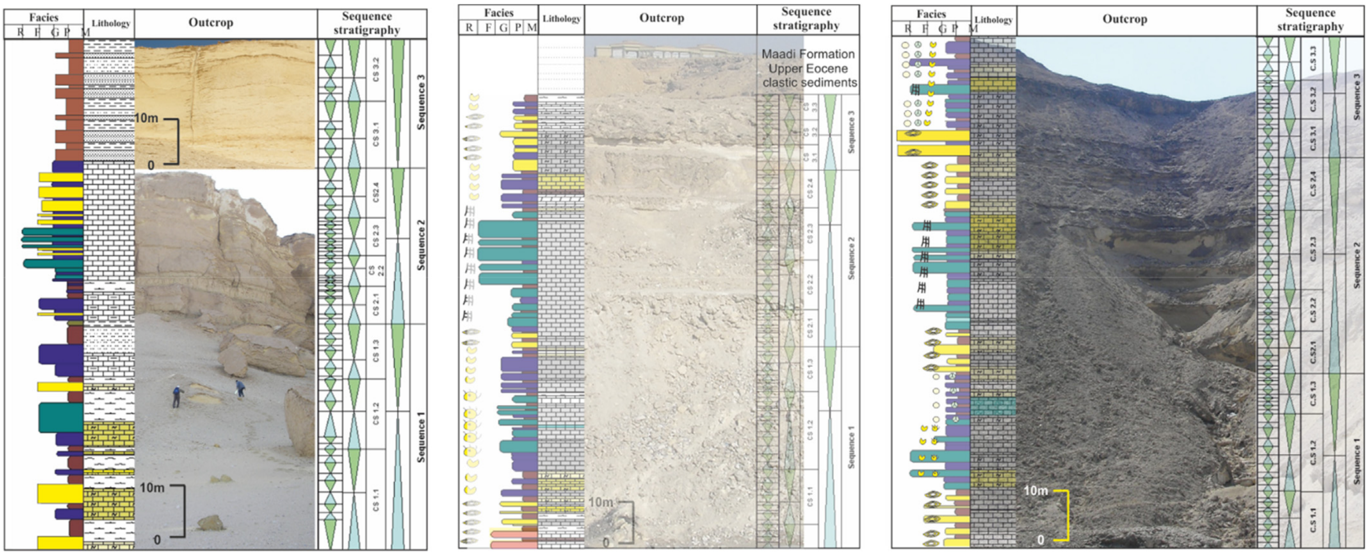

**Fig. 13.** Facies log and interpreted small-, medium- and large-scale cycles of the Qattamiya section, Mokattam section and Minqar el Rayan and Wadi el Hitan sections from right to left.

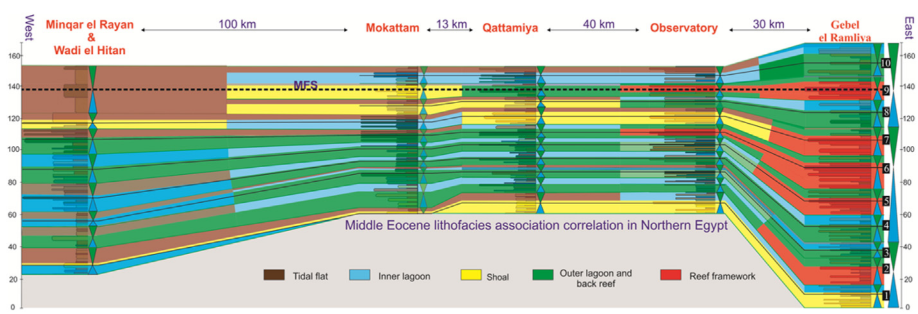

**Fig. 14.** Middle Eocene lithofacies association within chronostratigraphic cycle framework correlation.

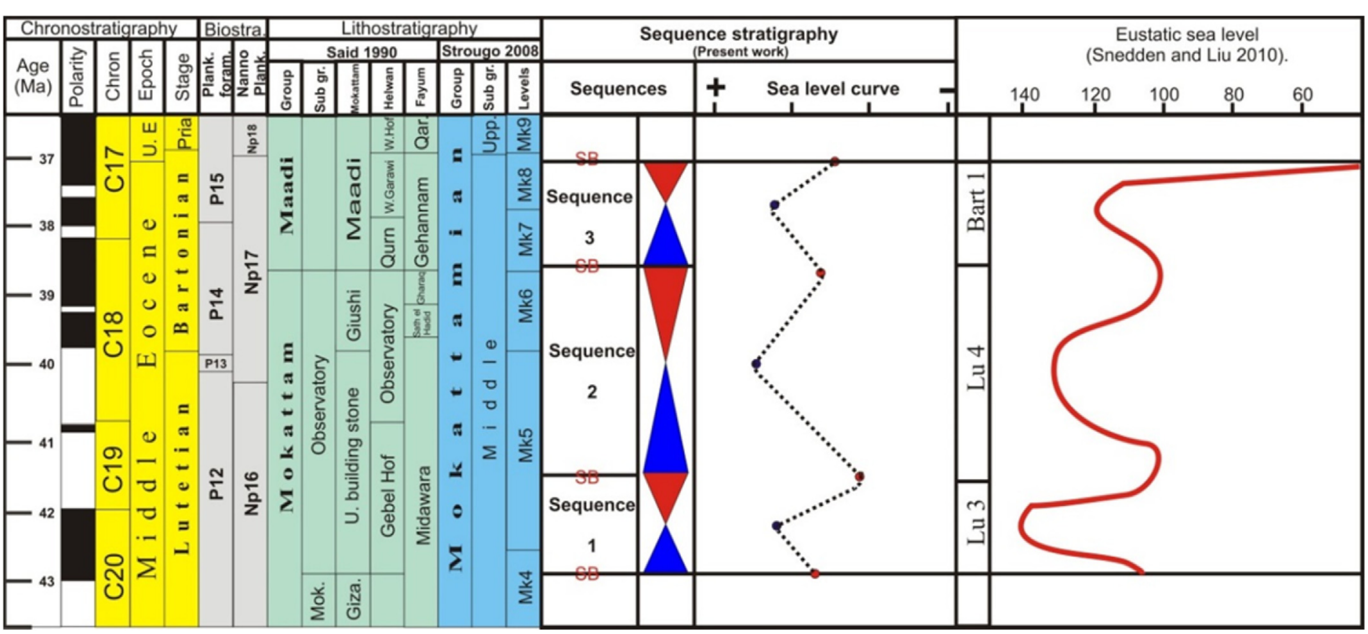

**Fig. 15.** The correlation chart of the lithostratigraphy shows identified sequences and sequence boundaries of the stack of the Middle Eocene studied sections compared with the global eustatic sea-level curve of Snedden and Liu (2010).

et al., 2012, Abuseda et al., 2015 and Sallam et al., 2015a,b). According to Strougo and Abd-Allah (1990) the sequence boundary between the Middle and the Upper Eocene is related to the earliest phase of tectonic activity prior to the initiation of the Gulf of Suez rift. Although tectonic activities may effect stratigraphic cyclicity at virtually any time scale (Catuneanu, 2006), high frequency cyclicity changes are also produced by the alterations in carbonate production rates or by the variable wave- and current-controlled sediment accumulation rates at changing water depths (e.g., James et al., 2001; Catuneanu and Elango, 2001; Davies and Gibling, 2003).

The hierarchy of cycles provides the key for the proposed correlation. The sequence boundaries of the medium-scale cycles are used as time lines. In this correlation, the medium-scale cycles are numbered, and traced from west to east, i.e. from landward (proximal) to seaward (distal). In general, the cycles exhibit different lithofacies types along the same time line. Based on the correlation, the western sections (e.g. Fayum area) represent tidal flat and lagoonal facies, the middle sections (e.g. Cairo area) represent a lagoonal and shoal facies, while eastern sections (e.g. Eastern Desert) represent reefal facies. A detailed analysis shows some intercalations between these lithofacies associations. Medium-scale cycle 1 is represented in all sections through inner lagoon lithofacies changing into shoals in the east. Medium-scale cycles 2, 3 and 4 show lateral changes from tidal flat sediments in the west to an inner lagoonal facies in the middle and a back-reef facies in the east. Medium-scale cycles 5, 6 and 7 show the lateral change from inner lagoonal facies in the west to an outer lagoon in the middle, and a coral build-up facies (reef flat lithofacies) in the east. Medium-scale cycles 8 and 9 show lateral changes from tidal flat in the east, to shoals and outer lagoonal sediment in the middle to coral build ups in the east. The last cycles show more proximal facies types grading from a leeward tidal flat lithofacies in the west to inner lagoonal and tidal flat sediments in the middle and an inner lagoonal facies in the east (Fig. 14).

As we see by the correlation, the widely changing thicknesses of sedimentary units and sedimentary features, traces of volcanic activities, or abrupt facies changes in the studies areas have not been observed, which implies that the change in the Middle Eocene rate of sea-level have been the primary control on facies, depositional environments and stratigraphic architecture (Pedley and Carannante, 2006, Nalin and Massari, 2009). Such inference is also supported by the plausible match of our detailed correlations with the global sea level curves of Haq (1988) and Snedden and Chengjie (2010) (Fig. 15).

It is also highly supported that, the extensive erosion, quarrying and the tectonic events - which break-up the different stratigraphic successions and create many grabens, half grabens, and horst blocks of variable sizes and amplitudes leaving a visible imprints on the studied stratigraphic sequences - are related to the post Middle Eocene tectonic movements (e.g. rifting of the Gulf of Suez, extension of the Red Sea, etc. see for example, Schlumberger, 1984; Young et al., 2000, Bosworth and McClay, 2001, Sehim et al., 2003 and El Atfy et al., 2014).

By the end of the Middle Eocene and the beginning of the Late Eocene, many fluvial distributaries have entered the depositional basin and a large thickness of cross bedded sandstone lithofacies has been formed, for example, in the Birket Qarun Formation in the Fayum and the Maadi Formation in Cairo, and that has been synchronous to the sea level fall (El-Fawal et al., 2013).

## 6. Conclusions

The overall sedimentary nature of the Middle Eocene studied sections between Wadi el Ramliya in the Eastern Desert near Sukhna city to Wadi el Hitan in the Western Desert in the Fayum area is dominated by shallow marine carbonates, and 19 different facies types were distinguished across a carbonate platform. These facies types were grouped into 5 lithofacies associations (LFA) ranging from a tidal flat to a reef framework, based on its position on the carbonate platform. These lithofacies types are stacked into 5 cycle types: These cycle types build up ten fourth-order cycle sets termed CS 1.1 to CS 3.3, which are vertically arranged in three third-order sequences (S1, S2 and S3). Lateral facies changes between the western sections (dominance of tidal flat and inner lagoonal associated facies), Cairo sections (dominance outer-lagoonal associated facies) and eastern sections (dominance of reefal associated facies) suggest a deepening trend towards the east. The documented sequence architecture shows a good match to the eustatic sea-level curve of Snedden and Chengjie (2010) during the Middle Eocene period. Therefore, the Middle Eocene sediments are likely controlled by eustasy rather than local and global tectonics.

## Acknowledgements

This work was funded by King Saud University, Deanship of Scientific Research, College of Science Research Center. The authors are grateful to Thomas Aigner (Tübingen University) for guiding, supporting, providing valuable suggestions, stimulating discussions and advice. I would especially like to thank Abdelmohsen Ziko (Zagazig University) and Mohram Elgamal (Petroleum Advisor) for supporting in the fieldwork, stimulating discussion and revising the manuscript.

## References

Abdel-Fattah, Z., Gingras, M., Caldwell, M., Permberton, S., 2010. Sedimentary environments and depositional characteristics of the middle to upper Eocene whale-bearing succession in the fayum depression, Egypt. Sedimentol 57, 446–476.

Abu Elghar, M., 2012. Sequence stratigraphy and cyclicity in the Middle Eocene of the Fayoum ranges, Western Desert, Egypt: implications for regional sea level changes. Mar. Petrol. Geol. 29 (1), 276–292.

Abuseda, H., Kassab, M.A., LaLa, A.M., El Sayed, N.A., 2015. Integrated petrographical and petrophysical studies of some Eocene carbonate rocks, Southwest Sinai. Egypt. Egypt. J. Petrol 24 (2), 213–230.

Adabi, M.H., Zohdi, A., Ghabeishavi, A., Amiri-Bakhtiyar, H., 2008. Applications of nummulitids and other larger benthic foraminifera in depositional environment and sequence stratigraphy: an example from the Eocene deposits in Zagros Basin, SW Iran. Facies 54 (4), 499–512.

Addi, A.A., 2015. Builders and taphonomic processes of bajocian coral patch reefs in the moroccan central high atlas. Arab. J. Geosci. 8, 8583–8600.

Aghaei, A., Mahboubi, A., Moussavi-Harami, R., Heubeck, C., Nadjafi, M., 2013. Facies analysis and sequence stratigraphy of an upper jurassic carbonate ramp in the eastern alborz range and binalud mountains, NE. Iran. Facies 59 (4), 863–889.

Aigner, T., 1985. Biofabrics as dynamic indicators in nummulite accumulations. J. Sediment. Res. 55 (1), 131–134.

Allam, A., Shama, K., Zalat, A., 1991. Biostratigraphy of the middle Eocene succession at mishgigah, Wadi Rayan, Libian Desert, Egypt. J.Afri. Earth Sci. 12 (3), 449–459.

Benisek, M.F., Betzler, C., Marcano, G., Mutti, M., 2009. Coralline-algal assemblages of a Burdigalian platform slope: implications for carbonate platform reconstruction (northern Sardinia, western Mediterranean Sea). Facies 55 (3), 375–386.

Bernau, J.M., Arnaud-Vanneau, A., Caus, E., 2003. Carbonate platform sequence stratigraphy in a rapidly subsiding area: the late barremian–early aptian of the organyà basin, Spanish Pyrenees. Sediment. Geol. 159, 177–201.

Blanchon, P., Jones, B., Ford, D.C., 2002. Discovery of a submerged 366 relic reef and shoreline off Grand Cayman: further support for an early Holocene jump in sea level. Sediment. Geol. 147 (3), 253–270.

Bosworth, W., McClay, K.R., 2001. Structural and stratigraphic evolution of the Gulf of Suez rift, Egypt: a synthesis. In: Zeigler, P.A., Cavazza, W., Robertson, A.H.F.R., Crasquin- Soleau, S. (Eds.), Peri-Tethys Memoir 6: Peri-Tethyan Rift/wrench Basins and Passive Margins, 186. Memoires du Museum National d'Histoire Naturelle de Paris, pp. 567–606.

Boukhary, M., Kamal, D., 1993. Nummulites praestriatus n. sp. from the Giushi member (biarritzian), Gebel Mokattam, greater Cairo, Egypt. Neues Jahrb. Fur Geol. UND Palaontologie Monatsh. 585–585.

Boukhary, M., Guernet, C., Strougo, A., Bassiouni, M., Bignot, G., Abdel Ghany, O., 1993. Eocene ostracods of mingar el-Rayan (fayum district, Egypt), stratigraphic

and paleogeographic implication. Rev. Micropaleont 36 (3), 191–211.
Bruggemann, J., Buffler, R., Guillaume, M., Walter, R., Cosel, R., Ghebretensae, B., Berhe, S., 2004. Stratigraphy, palaeoenvironments and model for the deposition of the Abdur Reef Limestone: context of an important archaeological site from the last interglacial on the Red Sea coast of Eritrea. Palaeogeogr. Palaeoclimatol. Palaeoecol. 203, 179–206.
Brunet, M., Wilmsen, M., Granath, J. (Eds.), 2009. South Caspian to Central Iran Basins. Geol. Soc, 312. Lond. Spec. Publ., p. 360
Cabioch, G., Montaggioni, L., Frank, N., Seard, C., Sallé, E., Payri, C., Paterne, M., 2008. Successive reef depositional events along the Marquesas foreslopes (French Polynesia) since 26 ka. Mar. Geol. 254 (1), 18–34.
Castro, J.M., De Gea, G.A., Ruiz-Ortiz, P.A., Nieto, L.M., 2008. Development of carbonate platforms on an extensional (rifted) margin: the Valanginian–Albian record of the Prebetic of Alicante (SE Spain). Cretac. Res. 29 (5), 848–860.
Catuneanu, O., 2006. Principles of Sequence Stratigraphy. Elsevier, Amsterdam, p. 375.
Catuneanu, O., Abreu, V., Bhattacharya, J., Blum, M., Dalrymple, R., Eriksson, P., Fielding, C., Fisher, W., Galloway, W., Gibling, M., Giles, K., Holbrook, J., Jordan, R., Kendall, C., Macurda, B., Martinsen, O., Miall, A., Neal, J., Nummedal, D., Pomar, L., Posamentier, H., Pratt, B., Sarg, J., Shanley, K., Steel, R., Strasser, A., Tucker, M., Winker, C., 2009. Towards the standardization of sequence stratigraphy. Earth Sci. Rev. 92, 1–33.
Catuneanu, O., Elango, H.N., 2001. Tectonic control on fluvial styles: the balfour formation of the Karoo basin, South Africa. Sediment. Geol. 140, 291–313.
Cross, T.A., Lessenger, M.A., 1998. Sediment volume partitioning: Rationale for stratigraphic model evaluation and high-resolution stratigraphic correlation. In: Sandvik, K.O., Gradstein, F., Milton, N. (Eds.), Predictive High-resolution Sequence Stratigraphy. Norweg. Petrol. Soc., Spec. Publ, pp. 171–196.
Davies, S., Gibling, M., 2003. Architecture of coastal and alluvial deposits in an extensional basin: the Carboniferous Joggins Formation of eastern Canada. Sedimentol 50, 415–439.
Egyptian geological survey, 1981. Geological Map of Egypt. http://library.wur.nl/isric/kaart/origineel/afr_egg.jpg. Accessed 03.09.10.
El Atfy, H., Brocke, R., Uhl, D., Ghassal, B., Stock, A.T., Littke, R., 2014. Source rock potential and paleoenvironment of the Miocene Rudeis and Kareem formations, Gulf of Suez, Egypt: an integrated palynofacies and organic geochemical approach. Intern. J. Coal Geol. 131, 326–343.
El Ayyat, A.M., 2013. Sedimentology, sequential analysis 409 and clay mineralogy of the lower Eocene sequence at Farafra Oasis area, Western Desert of Egypt. J. Afri. Earth Sci. 78, 28–50.
El-Azabi, M.H., 2006. Sedimentological characteristics, palaenvironments and cyclostratigraphy of the middle Eocene sequences in Gabal el-Ramliya, Maadi-Sukhna stretch, north eastern Desert. In: Egypt. 8th Int. Conf. on the Geology of Arab World (GAW 8). Cairo Univ., Egypt, pp. 1–31.
El-Fawal, F.M., El-Asmar, H.M., Sarhan, M.A.E.F., 2013. Depositional evolution of the middle- upper Eocene rocks, fayum area. Egypt. Arab. J. Geosci. 6 (3), 749–760.
Embry, A.F., 1993. Transgressive-regressive (TR) sequence analysis of the jurassic succession of the Sverdrup basin, canadian arctic archipelago. Canad. J. Earth Sci. 30 (2), 301–320.
Embry, A.F., Klovan, J.E., 1971. A late devonian reef tract on northeastern banks island, Northwest territories. Bull. Canad. Petrol.geol. 19, 730–781.
Fierstine, H.L., Gingerich, P.D., 2009. A Second and more complete Rostrum of Xiphiorhynchus aegyptiacus Weiler, 1929, (Perciformes: Xiphioidei: Xiphiidae: Xiphiorhynchinae), from the Birket Qarun Formation, upper Eocene. Egypt. J. verteb. Paleontol. 29 (2), 589–593.
Fursich, F., Wilmsen, M., Seyed-Emami, K., Schairer, G., Majidifard, M., 2003. Platform-basin transect of a middle to late jurassic large-scale carbonate platform system (Shotori mountains, Tabas area, East-Central Iran). Facies 48, 171–198.
Gingerich, P.D., 1992. Marine mammals (cetacea and Sirenia) from the Eocene of Gebel Mokattam and fayum, Egypt; stratigraphy, age and paleoenvironments. Univ. Mich. Pap. Paleontol. 30, 1–84.
Haggag, M.A., 1990. Globigerina Pseudoampliapertura 431 Zone, a New Late Eocene Planktonic Foraminiferal Zone (Fayoum Area, Egypt). N. Jah. Geol. Paläontol. Monat, Stuttgart, pp. 295–307.
Haggag, M.A., 1992. A comprehensive egyptian middle/upper Eocene Plancktonic foraminiferal zonation. Egypt. J. Geol. 36, 97–118.
Haq, B.U., 1988. Mesozoic and Cenozoic chronostratigraphy and cycles of sea-level change. SEPM Spec. Publ. 42, 71–108.
Helal, S.A., 1990. Stratigraphic and Paleontologic Studies of the Eocene Sediments in Gabel Shbraweet Area, Eastern Desert, Egypt. Msc. Thesis. Ain Shams Univ., p. 363
Helal, S.A., 2002. Contribution to the Eocene benthic foraminifera and ostracoda of the fayum depression. Egypt. Egypt. J. Paleontol. 2, 105–155.
Hottinger, L., 1997. Shallow benthic foraminiferal assemblages as signals for depth of their deposition and their limitations. Soc. Geol. Fr. Bull. 168, 491–505.
Issawi, B., 2002. Egypt during the Phanerozoic. Geol. Arab. World, Cairo Univ. 6th Int. Conf. 2, 401–450.
Issawi, B., 2005. Archean–Phanerozoic birth and development of the Egyptian land. 1st Int. Conf. Geol. Tethys Cairo Univ. 2 (380), 380–380.
Issawi, B., Francis, M., Youssef, A., Osman, R., 2009. The Phanerozoic of Egypt: a geodynamic approach. Geol. Surv. Egypt, Spec. Publ. 81, 589.
Issawi, B., Osman, R., 2002. Geological history of NE Egypt during the Paleozoic and Mesozoic as anticipated from lithofacies isopach maps. Geol. Arab World, Cairo Univ 6, 451–468.
James, N.P., Bone, Y., Collins, L.B., Kyser, T.K., 2001. Surficial sediments of the Great Australian Bight: facies dynamics and oceanography on a vast cool-water carbonate shelf. J. Sediment. Res. 71, 549–567.
James, N.P., Kobluk, D.R., 1978. Lower Cambrian patch reefs and associated sediments: southern Labrador, Canada. Sedimentol 25, 1–35.
Kerans, C., Tinker, S.W., 1997. Sequence Stratigraphy and Characterisation of Carbonate Reservoirs. In: Society of Economic Paleontologists and Mineralogists Short Course Notes, 40, p. 130.
Kovacs, J.S., 2005. Depth gradient proxies: palaeoecology versus sedimentology. Case study from the Turea Group deposits of the Paleogene Transylvanian Basin. Acta Palaeontol. Roman 5, 259–276.
Lotfy, H., Van der Voo, R., 2007. Tropical northeast Africa in the middle–late Eocene: paleomagnetism of the marine mammals sites and basalts in the Fayum province. Egypt. J. afri. Earth Sci. 47, 135–152.
Maanan, M., Zourarah, B., Carruesco, C., Aajjane, A., Naud, J., 2004. The distribution of heavy metals in the Sidi Moussa lagoon sediments (Atlantic Moroccan Coast). J. Afri. Earth Sci. 39 (3), 473–483.
Mansour, A.S., Holail, H.M., 2004. Dolomitization of middle Eocene carbonate rocks, Abu Roash area. Egypt. Carbonates evaporates 19 (2), 151–161.
Marzouk, A.M., El Shishtawy, A.M., Kasem, A.M., 2014. Calcareous nannofossil and planktonic foraminifera biostratigraphy through the middle to late Eocene transition of fayum area,Western Desert. Egypt. J. afri. Earth Sci. 100, 303–323.
Meckel, L.D., 1975. Holocene sand bodies in the California delta area, northern Gulf of Mexico. In: Broussard, M. (Ed.), Deltas, Models for Exploration. Houston Geol. Soc, pp. 239–266.
Mostafa, A., Hassan, A.M., 2004. Sequence stratigraphy and depositional history of some Mesozoic-Cenozoic succession in the Gulf of Suez and north Western Desert, Egypt. In: Proceed. 14th Symp. Phanerozoic and Development Egypt, pp. 27–58.
Moustafa, A.R., Khalil, M.H., 1989. North sinai structures and tectonic evolution. Middle east Research center, ain Shams University. Earth Sci. Ser. 3, 215–231.
Nakazawa, T., Ueno, K., 2004. Sequence boundary and related sedimentary and diagenetic facies formed on Middle Permian mid-oceanic carbonate platform: core observation of Akiyoshi Limestone, Southwest Japan. Facies 50 (2), 301–311.
Nalin, R., Massari, F., 2009. Facies and stratigraphic anatomy of a temperate carbonate sequence (Capo Colonna terrace, Late Pleistocene, southern Italy). J. Sediment. Res. 79 (4), 210–225.
Nichols, G., 1999. Sedimentology and Stratigraphy. Blackwell Sci. Pub., Oxford, London, Edinburgh, Melbourne, p. 355.
Omar, A.A., 1999. Benthic foraminifers of Wadi El Rayan, area, fayum province, Egypt(Stratigraphy and Paleoecology): GAW4. In: International Conference of the Arab World, Cairo Univ., Egypt, pp. 905–923.
Osman, R., 2003. New findings in the Eocene stratigraphy of Gebel ataqa–northern Galala, north Eastern Desert. Egypt. J. sedment. Egypt 11, 95–109.
Pedley, M., Carannante, G., 2006. Cool-water carbonate ramps: a review. Geol. Soc. London. Spec. Publ. 255 (1), 1–9.
Pomar, L., Hallock, P., 2007. Changes in coral-reef structure through the Miocene in the Mediterranean province: adaptive versus environmental influence. Geol. 35 (10), 899–902.
Racki, G., 1993. Evolution of the bank to reef complex in the devonian of the holy cross mountains. Acta Palaeontol. Polonica 37, 87–182.
Rasser, M.W., Scheibner, C., Mutti, M., 2005. A paleoenvironmental standard section for Early Ilerdian tropical carbonate factories (Corbieres, France; Pyrenees, Spain). Facies 51 (1–4), 218–232.
Sadeghi, R., Vaziri-Moghaddam, H., Taheri, A., 2011. Microfacies and sedimentary environment of the oligocene sequence (asmari formation) in Fars sub-basin, Zagros mountains, southwest Iran. Facies 57 (3), 431–446.
Said, R., 1990. The Geology of Egypt. Balkema, Rotterdam, p. 734.
Salem, R., 1976. Evolution of Eocene-Miocene sedimentation patterns in parts of northern Egypt. AAPG Bull. 60 (1), 34–64.
Sallam, E., Issawi, B., Osman, R., 2015a. Stratigraphy, facies, and depositional environments of the Paleogene sediments in Cairo–Suez district. Egypt. Arab. J. Geosci. 8 (4), 1939–1964.
Sallam, E., Wanas, H.A., Osman, R., 2015b. Stratigraphy, facies analysis and sequence stratigraphy of the Eocene succession in the Shabrawet area (north Eastern Desert, Egypt): an example for a tectonically influenced inner ramp carbonate platform. Arab. J.Geosci 1–26.
Schandelmeier, H., Reynolds, P., Semtner, A.K., 1997. Palaeogeographic-palaeotectonic Atlas of North-eastern Africa. Arabia and adjacent areas, Rotterdam, Balkema.
Schlumberger, 1984. In: Well Evaluation Conference, Egypt. Schlumberger Middle East SA, p. 201.
Sedgwick, P.E., Davis, R.A., 2003. Stratigraphy of washover deposits in Florida: implications for recognition in the stratigraphic record. Mar. Geol. 200 (1), 31–48.
Sehim, A., Ivankovic, J., Anis, W., Leustek, S., 2003. Regional structure setting of the Gulf of Suez. In: Oil and Gas Int. Conf., Zadar.
Selim, S.S., El Araby, A.A., Darwish, M., Kharadah, A.A., 2012. Anatomy and development of tectonically-induced Middle Eocene clastic wedge on the southern Tethyan Shelf. In: North Eastern Desert, Egypt. GeoConvention, pp. 1–6.
Shahin, A., Bassal, A., El Halaby, O., El Baz, S., 2007. Middle Eocene benthic foraminiferal biostratigraphy and paleoenvironment at the Qattamiya area, northern Eastern Desert. Egypt. Egypt. J. Paleontol. 7, 1–29.
Shen, J.W., Webb, G.E., Jell, J.S., 2008. Platform margins, reef facies, and microbial carbonates; a comparison of Devonian reef complexes in the Canning Basin, Western Australia, and the Guilin region, South China. Earth-Sci. Rev 88 (1),

33–59.
Snedden, J., Chengjie, Liu, 2010. A Compilation of Phanerozoic Sea-level Change, Coastal Onlaps and Recommended Sequence Designations. Search and discovery article no. 40594. www.searchanddiscovery.org.
Steckler, M.S., Berthelot, F., Lyberis, N., Le Pichon, X., 1988. Subsidence in the Gulf of Suez: implications for rifting and plate kinematics. Tectonophysics 153 (1), 249–270.
Strougo, A., 1985a. Eocene Stratigraphy of the Eastern Greater Cairo (Gebel Mokattam-helwan) Area. In: Earth Science Series, 5. Middle East Research Center, Ain Shams University, pp. 1–39.
Strougo, A., 1985b. Eocene Stratigraphy of the Giza Pyramids Plateau. In: Scientific Research Series, 5. Middle East Research Center, Ain Shams University, pp. 79–99.
Strougo, A., 2008. The Mokattamian Stage. In: Earth Science Series, 22. Middle East Research Center, Ain Shams University, pp. 47–108.
Strougo, A., Abd-Allah, A.M., 1990. Mokattamian Stratigraphy of North Central Eastern Desert (South of Maadi- Qattamiya Road). In: Earth Science Series, 4. Middle East Research Center, Ain Shams University, pp. 152–175.
Strougo, A., Bignot, G., Abd-Allah, A.M., 1992. Biostratigraphy and Paleoenvironments of Middle Eocene Benthic Foraminiferal Assemblages of the North Central Eastern Desert, Egypt. In: Earth Science Series, 6. Middle East Research Center, Ain Shams University, pp. 1–12.
Strougo, A., Boukhary, M.A., 1987. The middle Eocene–upper Eocene boundary in Egypt: present state of problem. Rev. Micropaleontol. 30, 122–127.
Strougo, A., Azab, M.M., 1991. Bivalve Molluscs from a Lower Mokattamian (Middle Eocene) Shell Bed at the Base of the Midawara Formation of Gebel El Mehasham, Magahaga Area. In: Earth Science Series, 5. Middle East Research Center, Ain Shams University, pp. 95–119.
Strougo, A., Faris, M., Haggag, M.A.Y., Abul-Nasr, R.A., Gingerich, P.D., 2013. Planktonic foraminifera and calcareous nannofossil biostratigraPhy through the middle to late Eocene transition at Wadi hitan, fayum Province, Egypt. Contributions Mus. Paleontol., Univ. Mich. 32 (8), 111–138.
Telford, P.G., 1988. Devonian Stratigraphy of the Moose River Basin, James Bay Lowland, Ontario, Canada. Proc. 2nd Int. Symp. Devonian System — Memoir 14 (1), 123–132.
Uhen, M.D., 2004. Form, Function, and Anatomy of Dorudon Atrox (Mammalian, Cetacean): an Archaeocete from the Middle to Late Eocene of Egypt. In: Papers of Palaeontology, 34. University of Michigan, p. 79.
Vaziri-Moghaddam, H., Kimiagari, M., Taheri, A., 2006. Depositional environment and sequence stratigraphy of the Oligo-Miocene Asmari Formation in SW Iran. Facies 52 (1), 41–51.
Young, M.J., Gawthorpe, R.L., Sharp, I.R., 2000. Sedimentology and sequence stratigraphy of a transfer zone coarse-grained delta, Miocene Suez Rift. Egypt. Sedimentology 47 (6), 1081–1104.
Zalmout, I., 2008. Late Eocene Sea Cows (Mammalia, Sirenia) from Wadi Al Hitan in the Fayum Basin, Egypt. PhD Thesis. University of Michigan, p. 382.
Zonneveld, J.P., Gingras, M.K., Pemberton, S.G., 2001. Trace fossil assemblages in a Middle Triassic mixed siliciclastic-carbonate marginal marine depositional system. British Columbia. Palaeogeogr. Palaeoclimatol. Palaeoecol 166 (3), 249–276.